UNIVERSIDAD DE INVESTIGACIÓN DE TECNOLOGÍA EXPERIMENTAL YACHAY

Escuela de Ciencias Matemáticas y Computacionales

TÍTULO: Application of topological optimization in 3 dimensions using radial basis functions

Trabajo de integración curricular presentado como requisito para la obtención del título de ingeniero en tecnologías de la información.

Autor:

Andrade Chamorro Eddy

Tutor:

Dr. Pineda Arias Israel

Urcuquí, Enero 2022

Urcuquí, 16 de diciembre de 2021

SECRETARÍA GENERAL
(Vicerrectorado Académico/Cancillería)
ESCUELA DE CIENCIAS MATEMÁTICAS Y COMPUTACIONALES
CARRERA DE TECNOLOGÍAS DE LA INFORMACIÓN
ACTA DE DEFENSA No. UITEY-ITE-2021-00037-AD

A los 16 días del mes de diciembre de 2021, a las 14:30 horas, de manera virtual mediante videoconferencia, y ante el Tribunal Calificador, integrado por los docentes:

Presidente Tribunal de Defensa	Dr. IZA PAREDES, CRISTHIAN RENE , Ph.D.
Miembro No Tutor	Dr. MANZANILLA MORILLO, RAUL , Ph.D.
Tutor	Dr. PINEDA ARIAS, ISRAEL GUSTAVO , Ph.D.

El(la) señor(ita) estudiante **ANDRADE CHAMORRO, EDDY RICARDO**, con cédula de identidad No. **1724145386**, de la **ESCUELA DE CIENCIAS MATEMÁTICAS Y COMPUTACIONALES**, de la Carrera de **TECNOLOGÍAS DE LA INFORMACIÓN**, aprobada por el Consejo de Educación Superior (CES), mediante Resolución **RPC-SO-43-No.496-2014**, realiza a través de videoconferencia, la sustentación de su trabajo de titulación denominado: **Application of topological optimization in 3 dimensions using radial basis functions**, previa a la obtención del título de **INGENIERO/A EN TECNOLOGÍAS DE LA INFORMACIÓN**.

El citado trabajo de titulación, fue debidamente aprobado por el(los) docente(s):

Tutor	Dr. PINEDA ARIAS, ISRAEL GUSTAVO , Ph.D.

Y recibió las observaciones de los otros miembros del Tribunal Calificador, las mismas que han sido incorporadas por el(la) estudiante.

Previamente cumplidos los requisitos legales y reglamentarios, el trabajo de titulación fue sustentado por el(la) estudiante y examinado por los miembros del Tribunal Calificador. Escuchada la sustentación del trabajo de titulación a través de videoconferencia, que integró la exposición de el(la) estudiante sobre el contenido de la misma y las preguntas formuladas por los miembros del Tribunal, se califica la sustentación del trabajo de titulación con las siguientes calificaciones:

Tipo	Docente	Calificación
Miembro Tribunal De Defensa	Dr. MANZANILLA MORILLO, RAUL , Ph.D.	10,0
Presidente Tribunal De Defensa	Dr. IZA PAREDES, CRISTHIAN RENE , Ph.D.	10,0
Tutor	Dr. PINEDA ARIAS, ISRAEL GUSTAVO , Ph.D.	9,0

Lo que da un promedio de: **9.7 (Nueve punto Siete)**, sobre 10 (diez), equivalente a: **APROBADO**

Para constancia de lo actuado, firman los miembros del Tribunal Calificador, el/la estudiante y el/la secretario ad-hoc.

ANDRADE CHAMORRO, EDDY RICARDO
Estudiante

EDDY RICARDO ANDRADE CHAMORRO
Firmado digitalmente por EDDY RICARDO ANDRADE CHAMORRO
Fecha: 2021.12.22 16:16:47 -05'00'

Dr. IZA PAREDES, CRISTHIAN RENE , Ph.D.
Presidente Tribunal de Defensa

Firmado electrónicamente por:
CRISTHIAN RENE IZA PAREDES

Dr. PINEDA ARIAS, ISRAEL GUSTAVO , Ph.D.
Tutor

Firmado electrónicamente por:
ISRAEL GUSTAVO PINEDA ARIAS

Dr. MANZANILLA MORILLO, RAUL , Ph.D.
Miembro No Tutor

Firmado electrónicamente por:
RAUL MANZANILLA

DAYSY MARGARITA MEDINA BRITO

Firmado digitalmente por DAYSY MARGARITA MEDINA BRITO
Fecha: 2021.12.21 08:25:24 -05'00'

MEDINA BRITO, DAYSY MARGARITA
Secretario Ad-hoc

AUTORÍA

Yo, **Eddy Ricardo Andrade Chamorro**, con cédula de identidad 1724145386, declaró que las ideas, juicios, valoraciones, interpretaciones, consultas bibliográficas, definiciones y conceptualizaciones expuestas en el presente trabajo; así cómo, los procedimientos y herramientas utilizadas en la investigación, son de absoluta responsabilidad de el autora del trabajo de integración curricular. Así mismo, me acojo a los reglamentos internos de la Universidad de Investigación de Tecnología Experimental Yachay.

Urcuquí, enero 2022.

EDDY RICARDO ANDRADE CHAMORRO

Firmado digitalmente por EDDY RICARDO ANDRADE CHAMORRO
Fecha: 2022.01.06 03:50:25 -05'00'

Eddy Ricardo Andrade Chamorro
CI: 1724145386

AUTORIZACIÓN DE PUBLICACIÓN

Yo, **Eddy Ricardo Andrade Chamorro,** con cédula de identidad 1724145386, cedo a la Universidad de Investigación de Tecnología Experimental Yachay, los derechos de publicación de la presente obra, sin que deba haber un reconocimiento económico por este concepto. Declaro además que el texto del presente trabajo de titulación no podrá ser cedido a ninguna empresa editorial para su publicación u otros fines, sin contar previamente con la autorización escrita de la Universidad.

Asimismo, autorizo a la Universidad que realice la digitalización y publicación de este trabajo de integración curricular en el repositorio virtual, de conformidad a lo dispuesto en el Art. 144 de la Ley Orgánica de Educación Superior

Urcuquí, enero 2022.

EDDY RICARDO ANDRADE CHAMORRO

Firmado digitalmente por EDDY RICARDO ANDRADE CHAMORRO
Fecha: 2022.01.06 03:50:42 -05'00'

____

Eddy Ricardo Andrade Chamorro
CI: 1724145386

Dedication

"This graduation project is gratefully dedicated to my parents Olger and Amparo. Thanks for your great support and continuous care."

Acknowledgments

The completion of this project could not have been possible without the guidance and expertise of Prof. Israel Pineda. PhD. We would also thanks to Prof. Raul Manzanilla. PhD. who collaborated in the review and resolution of key obstacles to finalize this work.

Abstract

Human intuition has driven the evolution of mechanical design to maximize performance and minimize production costs. In the last decades, computer-aided design approaches have improved the mechanical design process, introducing innovative methods and new optimization dimensions. Currently, these approaches allow highly customizable designs and great weight savings but are typically constrained to small sizes and low resolutions. The huge computational complexity presented by optimal designing is due to the large number of variables involved. As a result, designing optimal large structures requires huge computational resources. Nowadays, the need for efficient mechanisms and therefore efficient energy consumption has been highlighted by the United Nations within the framework of sustainable development. This has highlighted the development and research of new and better optimization techniques that allow designing and manufacturing high-performance components.

PLSM based topology optimization method is based on the mathematical simplification of a Hamilton-Jacobi partial differential equation (PDE) into a more convenient ordinary differential equations (ODEs) system. This simplification is reached through parameterizing the level set function using radial basis functions (RBFs). These functions, popular in scattered data fitting and function approximation, are incorporated into the conventional level set methods to represent the surface through implicit modeling. The RBF used in this work was a multiquadric (MQ) spline due to its smooth feature and performance. The parameterization using MQ spline allows to define the implicit level set function with a high level of accuracy and smoothness. Mainly, the parameterization allows transforming the original time-dependent initial value to an interpolation problem for the initial values of the generalized expansion coefficients. Additionally, a physically meaningful and efficient extension velocity method is used to avoid possible problems caused by not implementing a full reinitialization scheme.

The result of this work is a MATLAB code to perform topology optimization of a 3-dimensional body within the framework of minimization of compliance. In this code, the supports and loads, as well as the number of elements in which the object is discretized can be customized. Several numerical examples in three dimensions are presented to demonstrate the effectiveness of our implementation. Finally, a benchmark is presented comparing the results obtained by our implementation with the results presented by other methods as well as other PLSM implementations.

Keywords: Topology, Optimization, Compliance, MATLAB.

Resumen

La intuición humana ha impulsado la evolución del diseño mecánico para maximizar el rendimiento y minimizar los costos de producción. En las últimas décadas, los enfoques de diseño asistido por computadora han mejorado el proceso de diseño mecánico, introduciendo métodos innovadores y nuevas dimensiones de optimización. Actualmente, estos enfoques permiten diseños altamente personalizables y grandes ahorros de peso, pero generalmente se limitan a tamaños pequeños y resoluciones bajas. La enorme complejidad computacional que presenta el diseño óptimo se debe a la gran cantidad de variables involucradas. Como resultado, diseñar grandes estructuras óptimas requiere enormes recursos computacionales. En la actualidad, la necesidad de mecanismos eficientes y, por tanto, de un consumo energético eficiente ha sido destacada por Naciones Unidas en el marco del desarrollo sostenible. Esto ha destacado el desarrollo e investigación de nuevas y mejores técnicas de optimización que permiten diseñar y fabricar componentes de alto rendimiento.

El método de optimización de topología basado en PLSM se basa en la simplificación matemática de una ecuación diferencial parcial (PDE) de Hamilton-Jacobi en un sistema de ecuaciones diferenciales ordinarias (ODE) más conveniente. Esta simplificación se alcanza mediante la parametrización de la función de conjunto de niveles utilizando funciones de base radial (RBF). Estas funciones, populares en el ajuste de datos dispersos y la aproximación de funciones, se incorporan en los métodos de conjuntos de niveles convencionales para representar la superficie a través del modelado implícito. El RBF utilizado en este trabajo fue un spline multicuadrico (MQ) debido a su característica y rendimiento suaves. La parametrización mediante MQ spline permite de fi nir la función de ajuste de nivel implícito con un alto nivel de precisión y suavidad. Básicamente, la parametrización permite transformar el valor inicial dependiente del tiempo original en un problema de interpolación para los valores iniciales de los coeficientes de expansión generalizados. Además, se utiliza un método de velocidad de extensión físicamente significativo y eficiente para evitar posibles problemas causados por no implementar un esquema de reinicialización completo.

El resultado de este trabajo es un código MATLAB para realizar la optimización topológica de un cuerpo tridimensional dentro del marco de minimización del cumplimiento. En este código se pueden personalizar los soportes y cargas, así como la cantidad de elementos en los que se discretiza el objeto. Se presentan varios ejemplos numéricos en tres dimensiones para demostrar la efectividad de nuestra implementación. Finalmente, se presenta un benchmark comparando los resultados obtenidos por nuestra implementación con los resultados presentados por otros métodos así como otras implementaciones PLSM.

Palabras Clave: Topologia, Optimización, Cumplimiento, MATLAB.

Contents

List of Tables

List of Figures

Chapter 1

Introduction

1.1 Background

Structural topology optimization is one of the most important structural optimization methods because of its ability in achieving greatest saving. Structural topology optimization is a mathematical method that optimizes the material layout within a given design space, for a given set of loads, boundary conditions and constraints with the goal of maximizing the performance of the system. Topology optimization by distribution of isotropic material. Material distribution method for finding the optimum layout of linearly elastic structure. Layout of the structure includes information on the topology, shape and sizing of the structure and the material distribution method allows for addressing all three problems simultaneously. In a typical sizing problem the goal may be to find the optimal thickness distribution of a linearly elastic plate or the optimal member areas in a truss structure. The optimal thickness distribution minimizes a physical quantity such as the mean compliance, peak stress, deflection. The design variable is the thickness of the plate and the state variable may be its deflection. The main feature of the sizing problem is that the domain of the design model and state variables is known a priori and is fixed throughout the optimization process. On the other hand, in a shape optimization problem the goal is to find the optimum shape of this domain, that is, the shape problem is defined on a domain which is now the design variable. Topology optimization of solid structures involves the determination of features such as the number and location and shape of holes and the connectivity of the domain [1].

The purpose of topology optimization is to find the optimal layout of a structure within a specified region. The only known quantities in the problem are the applied loads, the possible support conditions, the volume of the structure to be constructed and possibly some additional design restrictions such as the location and size of the prescribed holes or solid areas.

The topology, shape and size of the structure are not represented by standar parametric functions but by a set of distributed functions defined on a fixed design domain. These functions in turn represent a parametrization of the stiffness tensor of the continuum and it is a suitable choice of this parametrization which led to the proper design formulation for topology optimization [1].

Topological optimization has been recognized as one of the most important structural optimizations due to its ability to achieve significant material savings. However, topological optimization has been identified as one of the most challenging tasks in structural design. For topology and shape optimization problems, a common approach is using level set methods. These methods calculate and analyze the movement of an interface in two or three dimensions. This interface can easily develop sharp corners, split, and merge, allowing the level set method to have a wide range of applications.

The proposal is to implement a high performance algorithm to solve applications of 3-dimensional topology optimization based on parameterized level set method using radial basis functions (RBF). In the parameterized level set method, the level set function is decoupled by a linear combination of a set of radial basis functions and coefficients. Since the radial basis functions are only related to spatial coordinates, the evolution of the level set is transformed into an update of the coefficients of expansion of the radial basis functions. Topology optimization in actual applications requires huge computing and storage resources. Due this, the research on this topic is limited to small objects with low resolution and the use of sparse matrices is mandatory.

1.2 Problem Statement

Structural optimization maximizes the performance of mechanical components used in industries ranging from health to transport. However, due to huge computational resources required, its applicability is constrained to the design of simple and small structures. Recently, state-of-the-art methods with giga-voxel resolution have provided insights into the optimal distribution of material within structures in the range of decameters [7].

Aage *et al.* [7] presented a giga-voxel computational morphogenesis tool that was able to design the internal structure of a full-scale aeroplane wing. The optimized design reached unprecedented structural detail ranging from tens of meters to millimetres and reached a mass reduction of 5 per cent. This mass reduction translates into a reduction in fuel consumption of up to 200 tons per year per aeroplane [8]. According to the World Bank [9] the aviation industry had produced 11.65Gt CO_2 representing 21.5% of global GHGs emissions in 2021.

Optimally designed components have a major impact on the performance of the system of which they are part. Going from a reduced manufacturing cost, weight reduction, and more efficient use of energy and consequently of the fuel used. This is the case of the means of maritime, land, and mostly air transport.

The Institute for Energy and Environmental Research has made several updates on its research on energy savings by light-weighting [10] [11] [8]. In this research, the relationship between weight and energy consumption of different means of transport is studied. In the update released in 2016, Helms and Krack [12] raised the impact on energy consumption, and consequently on combustion and CO_2 emissions that would produce a certain reduction in weight. The authors determined that lifetime CO_2 saving potential can be up to 22 tons of CO_2 per 100 kg of reduced weight for a given type of vehicle. This demonstrates the importance of developing high-performance component manufacturing methods to reduce the environmental impact of the transportation industry on the environment. The manufacturing of transportation components has been seen as an emerging response to the SDG agenda. Kaitano and Nhamo [13] presented the approaches considered by companies that manufacture aircraft in their article Major Global Aircraft Manufacturers and Emerging Responses to the SDGs Agenda.

One of the current approaches to manufacturing high-performance components is through topological optimization. This approach allows designing optimal and light structures, with high mechanical performance. Topological optimization has been recognized as one of the most important structural optimizations due to its ability to achieve significant material savings. However, topological optimization has been identified as one of the most challenging tasks in structural design. For topology and shape optimization problems, a common approach is using level set methods. These methods calculate and analyze the movement of an interface in two or three dimensions. This interface can easily develop sharp corners, split, and merge, allowing the level set method to have a wide range of applications.

In this work an implementation of 3-dimensional parameterized level method for structural topological optimization is proposed. This method is implemented within the optimal topological framework of minimum compliance. Topological optimization based on the parameterized level set method is being studied extensively due to the feasibility of manufacturing the optimal designs that this method produces. One of the most widespread topological optimization methods is the SIMP (Solid Isotropic Material with Penalization) method due to its ease of implementation and low consumption of computational resources. However, the optimal designs produced by this method feature zigzag geometries due to intermediate densities. On the other hand, PLSM-based methods have been coupled to additive manufacturing processes due to the geometry they generate [14].

1.3 Objectives

1.3.1 General Objective

Implement an algorithm to perform structural topological optimization within the framework of minimizing compliance and with a volume restriction based in the parameterized level set method to three-dimensional objects.

1.3.2 Specific Objectives

- Implement an efficient algorithm to minimizing the compliance of a body subject to loads and supports.
- Make loads and supports configurable.
- Display the optimization process in real-time.
- Carry out a comparison between the optimal designs obtained with the proposed implementation and with the designs obtained through implementations reported in the literature.
- Develop the algorithm within the framework of vector processing to achieve optimal performance.

Chapter 2

Theoretical Framework

2.1 Structural Optimization

Structural optimization includes three optimization features; these are optimization of size, shape, and topology. In structural optimization problems, state and design variables can be defined. State variables can represent the complete dynamic state of the object at a given moment, while design variables can be modified to define an optimal design. This section follows the organization of Bendsoe and Sigmund [1] in their work Topology Optimization Theory, Methods, and Applications.

In a size optimization problem, the objective is to find the optimal thickness distribution of a linearly elastic plate. The optimal thickness distribution minimizes a physical quantity such as the mean compliance, peak stress, and deflection. The design variable is the thickness of the plate and the state variable could be its deflection. The main characteristic of the size optimization problem is that the domain of the design model and the state variables are known *apriori* and do not change during the entire optimization process. On the other hand, in a shape optimization problem, the goal is to find the optimal shape. The topology optimization of solid structures involves the determination of characteristics such as the number, location, and shape of holes and the connectivity of the domain.

Structural topology optimization is one of the most important structural optimization methods due to the efficient use of material that it reaches. Structural optimization is a mathematical method that optimizes the arrangement of material within a given design domain and for a set of specific constraints and conditions. These restrictions can be several loads, boundary conditions, and volume restrictions. The goal of structural topological optimization is to maximize the structural performance of an object.

The topology, shape, and size of the structure are not represented by a standard parametric function but by a set of distributed functions defined in a fixed design domain. These functions represent a parameterization of the stiffness tensor and it is a feasible choice of its parameterization, which leads to a suitable formulation for topological optimization. This work studies the minimization of compliance.

The general framework for optimal shape design is formulated as a material distribution problem. The configuration is similar to the formulations for size problems for discrete and continuous structures. The type of problem being considered is from an inherently large-scale computational point of view, both in state and in design variables.

Considering a mechanical element as a body occupying the domain Ω^{mat} which is part of a larger reference domain Ω in $\mathbb{R}^2$ or $\mathbb{R}^3$. The reference domain is chosen in such a way that it allows a definition of applied loads and boundary conditions. Referring to reference domain Ω the optimal design problem can be defined as the problem of finding the optimal choice of the stiffness tensor $E_{ijkl}(x)$ which is variable over the domain. The problem of minimum compliance or maximum overall stiffness has the form:

$$\min_{u\epsilon U,E} \quad l(u) \tag{2.1a}$$

$$\text{subject to} \quad a_E(u,v) = l(u), \text{ for all } v\epsilon U, \tag{2.1b}$$

$$E\epsilon E_{a,d}, \tag{2.1c}$$

where the load lineal form $l(u)$ of the stiffness tensor $E_{ijkl}(x)$ with linearized strains $\varepsilon_{ij}(u) = \frac{1}{2}(\frac{\partial_{u_i}}{\partial_{x_j}} + \frac{\partial_{u_j}}{\partial_{x_i}})$, is:

$$l(u) = \int_\Omega fud\Omega + \int_{\tau_T} ds. \tag{2.2}$$

The bilinear form of energy (i.e. internal virtual work of an elastic body in equilibrium u and for an arbitrary virtual displacement v) of the stiffness tensor $E_{ijkl}(x)$ takes the form:

$$a(u,v) = \int_\Omega E_{ijkl}(x)\varepsilon_{ij}(u)\varepsilon_{kl}(v)d\Omega. \tag{2.3}$$

In the Equation 2.4a the equilibrium equation can be written in its weak form, the variational form, with U denoting the space ok kinematically admisible displacements, f are the forces on the body and t are the border tractions in the part of the traction. Note that the index E is used to indicate that the bilinear form a_E it depends on the design variables.

In the Ecuation 2.4a, E_{ad} denotes the set of allowable stiffness tensors for the design problem. In the case of topological design, E_{ad} could, consist of all the stiffness tensors that achieve the material properties for a given isotropic material in the set Ω^{mat} and zero properties anywhere else.

When solving problems of the type shown in Equation 2.4a by computational means, it is common to discretize the problem using finite elements. It is important to note that there are two fields of interest in 2.4a, these being the displacement u and stiffness E. If the same finite element mesh is used for both fields and discretized E as constant in each element, we can write the discrete form of 2.4a as:

$$\min_{u\epsilon U,E_e} \quad f^T u \tag{2.4a}$$

$$\text{subject to} \quad K(E_e)u = f, \tag{2.4b}$$

$$E\epsilon E_{a,d}, \tag{2.4c}$$

here u and f are the displacement vectors and loads, respectively. The stiffness matrix K depends on the element stiffness e E_e. K can be written in the form:

$$\mathbf{K} = \sum_{e=1}^{N} \boldsymbol{K}_e(E_e). \tag{2.6}$$

where K_e is the element stiffness matrix.

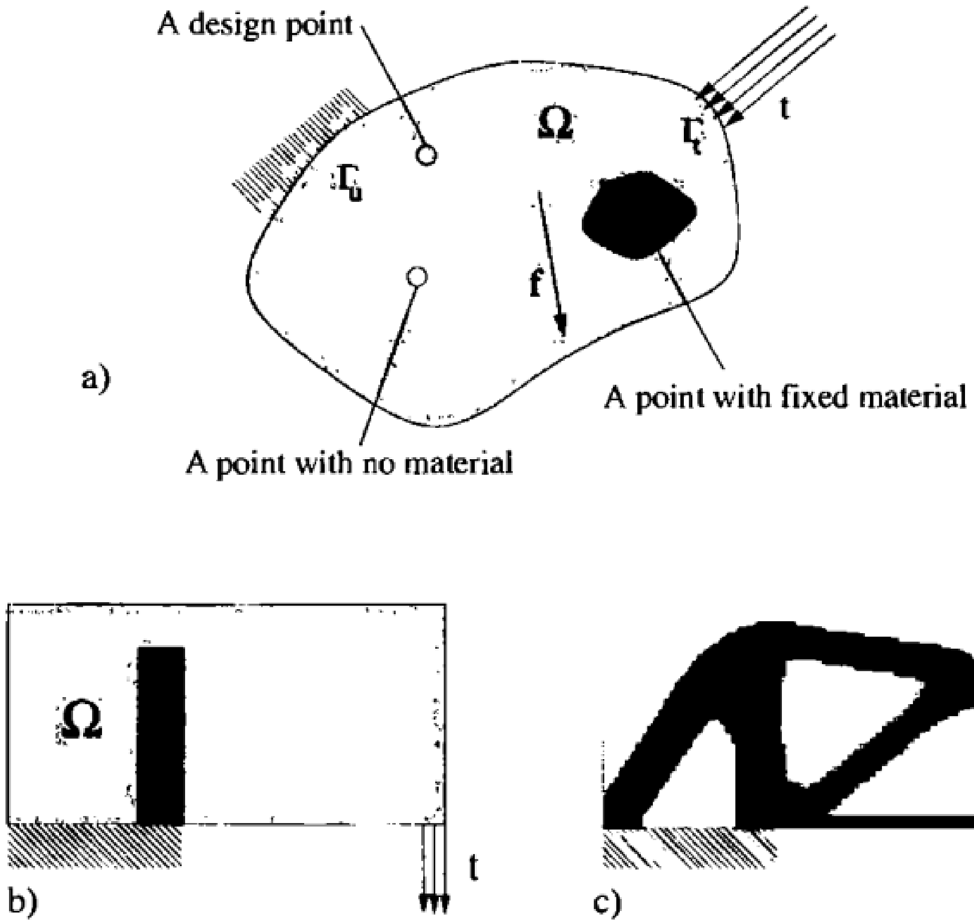

Figure 2.1: a) The generalized shape design problem of finding the optimal material distribution in a two-dimensional domain. b) Example rectangular design domain and c) topology optimized solution based on a 3200 element discretization and 50% material volume. Source: [1]

2.2 Topology Optimization Based on Level Set Method

The family of methods based on the implicit moving interfaces using the level set methods has been widely studied. The level method first introduced by Osher and Sethian [15] is a versatile method for tracking the evolution of dynamic interfaces in two or three dimensions. The level set method has a wide range of applications since the tracked interfaces may break apart and merge together. A level set-based topology optimization method combined with the shape derivative is proposed. This family of methods based on the level set has the attractive feature that it can always provide clear boundary and geometry information during the optimization process. In topology optimization, the level set function $\Phi(x)$, which is Lipschitz-continuous, represents the surface implicitly. The surface itself is the zero isosurface $\boldsymbol{x}\epsilon\mathbb{R}^d|\Phi(\boldsymbol{x}) = 0$ where d can takes the values $d = 2, 3$. The time evolution of the surface can be described by the PDEs involving $\Phi(x)$. The shape and topology of the structure are described by a level set function $\Phi(x)$ defined as:

$$\Phi(\mathbf{x}) = 0 \forall \mathbf{x} \in \partial\Omega \cap D, \tag{2.7a}$$
$$\Phi(\mathbf{x}) < 0 \quad \forall \mathbf{x} \in \Omega \setminus \partial\Omega, \tag{2.7b}$$
$$\Phi(\mathbf{x}) > 0 \; \forall \mathbf{x} \in (D \setminus \Omega). \tag{2.7c}$$
$$\tag{2.7d}$$

Where $D \subset \mathbb{R}^d$ is a fixed design domain in which all admissible designs Ω are included [16].

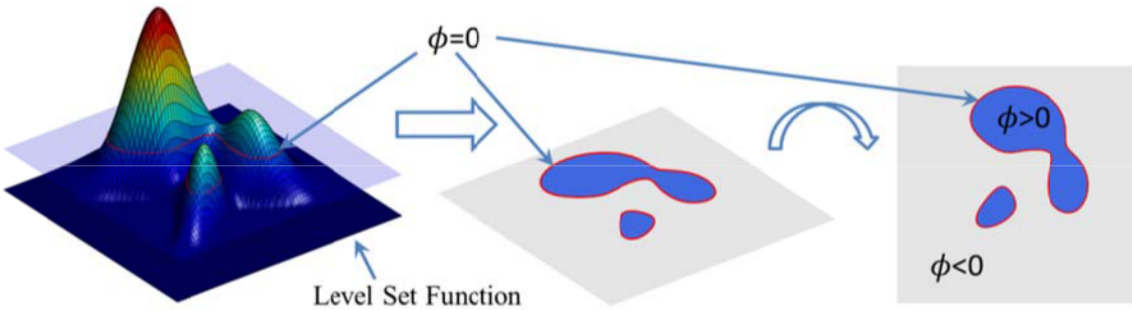

Figure 2.2: Level set function representation. Source: [2]

The following expression of the normal velocity is used as the advection velocity in the following Hamilton-Jacobi Equation

$$V_n = \mathbf{V}\left(-\frac{\nabla\Phi}{|\nabla\Phi|}\right), \tag{2.8}$$

$$\frac{\partial\phi}{\partial t} - V_n\,|\nabla\phi| = 0. \tag{2.9}$$

Where $\nabla(\phi)$ denotes the spatial gradient of the ϕ function, t is the pseudo time representing the evolution in time of the level set function, and $V_n = V_{\mathbf{x},t}$ is the normal velocity used as advection velocity chosen towards outside.

The conventional level set requires a reinitialization scheme to maintain a signed distance function by using a PDE-based method as the presented by Peng [17]. The reinitialization procedure keeps the norm of the gradient of the level set function constant and allows a stable evolution.

Another issue of the conventional level set method is the appropriate choice of finite element methods on a fixed Cartesian grid to solve the Hamilton Jacobi Partial Differential Equation PDE. A general framework involves an upwind differencing scheme, a reinitialization procedure, and velocity extension.

The time step size must be sufficiently small to satisfy the Courant-Friedrichs-Lewy (CFL) condition for numerical stability. This condition states that the ratio of the spatial discretization to the time discretization must be at least as large as the largest velocity which signals propagate in solutions of the partial differential equation. It indicates that the largest time step cannot be larger than the ratio of the minimum grid interval to the magnitude of the velocity. Furthermore, the CFL condition may limit the numerical step size.

The conventional level set method lacks the capacity to generate new holes inside the design domain which makes it difficult to reach the global optimum. Instead, the method is prone to get stuck in local minimum.

Level Set Method Limitations

In conventional topological optimization based on the level set method, a general analytical function for $\Phi(t, \mathbf{x})$ is not known. So it must be discretized for level set processing, often through a distance transformation. In a Eulerian approach, a numerous procedure for solving the partial differential equation of the Hamilton Jacobi type is indispensable. This procedure requires an appropriate choice of an upwind scheme, extension rates, and reset algorithms, which could limit the usefulness of the level set method.

Re-initialization prevents the level set function from nucleating holes within the material regions [18] [19]. Another important limitation lies in the discrete representation. In the Eulerian approach, the transport Equation 2.9 is solved with a finite difference or finite elements on a fixed grid or mesh. One of the key steps in the Eulerian approach is to describe the geometry or topology using the nodal values from $\Phi(\mathbf{x})$ and shape functions to ensure that the space of feasible designs will be smooth enough in shape [15] [20]. In practice, only low-order approximations as functions of form C^0 are used due to polynomial snaking problem [21] that high-dimensional polynomial interpolation can easily lead to singular problems and cause very poor derivative estimates. Also, only the implicit function $\Phi(\mathbf{x})$, instead of their partial derivatives they can be guaranteed continuous throughout the mesh.

A better method is to retain the topological benefits of the implicit representation of a level set model while avoiding the drawbacks of using its discrete samples on a fixed mesh or grid. The level set method parameterized $\Phi(t, \mathbf{x})$ to include alternative representations to the implicit representation which provides a free form representation with parameterization. To this end, the level set method using RBF radial basis functions is developed for structural topological optimization.

By using the RBF functions and modeling, global smoothness of the implicit function can be achieved, therefore, the precision and efficiency of the level set method is significantly improved. The parameterization of the implicit model converts the Hamilton Jacobi partial differential equation into a more mathematically convenient system of ordinary differential equations ODEs. Additionally, resetting becomes unnecessary, which could allow nucleation of new holes.

Summarizing, conventional level set method does not present a hole nucleation mechanism if the Hamilton-Jacobi equation is solved under strict conditions for numerical stability [22], [23]. Furthermore, the Hamilton Jacobi equation satisfies a maximum principle and reinitialization must be applied to ensure the regularity of the level set function thus preventing the generation of new holes within the design domain [23] , [24].

2.3 Radial Basis Function Implicit Modeling

To model and reconstruct all the allowable design with a single function which is globally continuous and differentiable, an implicit modeling method based on radial basis functions is employed. RBFs are popular for interpolating sparse data to produce edges and smooth surfaces as the associated system of nonlinear equations is guaranteed to be invertible under stable conditions at the data point locations [25]. RBF functions have been shown to be effective when the function to be approximated is multiple variables, or is given only by a large amount of data. In real-world applications, radial vase function techniques have become extremely useful, shifting from pattern reconstruction to artificial intelligence [26]. Implicit RBF modeling is used as an effective representation method to reconstruct the shape and topology of an allowable design.

Radial basis functions are radially symmetric functions centered on particular points, or nodes, which can be expressed as follows:

$$\varphi_i(\mathbf{x}) = \varphi(\|\mathbf{x} - \mathbf{x_i}\|), \mathbf{x}_i \in D \tag{2.10}$$

where $\|.\|$ denotes the Euclidean norm $\mathbb{R}^d$ [27], and $\mathbf{x}_i$ is the position knot. Only a fixed function forms $\varphi : \mathbb{R}^+ \to \mathbb{R}$ with $\varphi(0) \geq 0$ is used as basis to form a family of independent functions. There are a wide class of radial basis functions. The commonly used functions includes thin plate spline, splines polyharmonic splines, multiquadratic, and compactly supported. Among the most common, the multiquadratic function has the best performance and can be written as:

$$\varphi_i(\mathbf{x}) = \sqrt{(\mathbf{x} - \mathbf{x}_i)^2 + c_i^2} \tag{2.11}$$

where c_i is the free from parameter which is commonly assumed constant for all i in most applications [27]. Figure 2.3 shows the multiquadratic function centered at the original point with two different free form parameters 1 and 0.0001. It can be noted that a larger shape parameter leads to a flatter shape which is less sensitive to the difference in radial distance. It should be noted that $\varphi_i(\mathbf{x})$ in equation 8 it is continuously differentiable, so that the multiquadratic functions are infinitely smooth [28]. The conditional positive definition of multi-square placement matrices has been proven by Micchelli [29]. The multi quadratic functions were ranked as the best in interpolations by Franke [30].

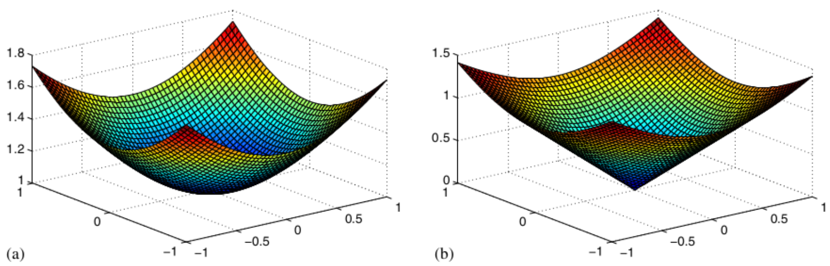

Figure 2.3: Multiquadratic spline: (a) $c = c_{i=1}$; y (b) $c = c_i = 0.0001$. Source: [2]

MQ functions are used to interpolate scalar functions $\Phi(\mathbf{x})$ with N knots using N functions MQ centereds at these knuts. The interpolant resulting from the implicit function can be written as:

$$\Phi(\mathbf{x}) = \sum_{i=1}^{N} \alpha_i \varphi_i(\mathbf{x}) + p(\mathbf{x}) \tag{2.12}$$

where α_i is the weight or generalized coefficient of expansion of the radial basis function positioned at the i th node, $p(\mathbf{x})$ is a polynomial of the first degree to consider the linear and constant portions of $\Phi(\mathbf{x})$ and to ensure the positive definition of the solution [31]. For three-dimensional modeling problems, $p(\mathbf{x})$ can be given by:

$$p(\mathbf{x}) = p_0 + p_1 x + p_2(y) + p_3 z. \tag{2.13}$$

In which p_0, p_1,p_2 are p_3 are the coefficients of the polynomial $p(\mathbf{x})$. Due to the introduction of this polynomial, to ensure a unique solution, the RBF interpolant of $\Phi(\mathbf{x})$ in the Equation 2.12 must be subject to the following orthogonality constraints [28] [25] [31] [32]:

$$\sum_{i=1}^{N} \alpha_i = 0; \sum_{i=1}^{N} \alpha_i x_i = 0; \sum_{i=1}^{N} \alpha_i y_i = 0; \sum_{i=1}^{N} \alpha_i z_i = 0. \tag{2.14}$$

If the values of the interpolation data $f_1, \cdots, f_N \in \mathbb{R}$ at the location of the knots $\mathbf{x}_1, \cdots, \mathbf{x}_N \in \Omega\mathbb{R}^d$ are given, the RBF interpolate of $\Phi(\mathbf{x})$ in Equation 2.12 can be obtained by solving the system of $N+4$ linear equations for $N+4$ unknown coefficients of expansion:

$$\Phi(\mathbf{x}_i) = f_i, i = 1, \cdots, N \sum_{i=1}^{N} \alpha_i = 0; \sum_{i=1}^{N} \alpha_i x_i = 0; \sum_{i=1}^{N} \alpha_i y_i = 0; \sum_{i=1}^{N} \alpha_i z_i = 0; \tag{2.15}$$

That can be written in matrix form:

$$\mathbf{H}\alpha = \mathbf{f} \tag{2.16}$$

where:

$$\mathbf{H} = \begin{bmatrix} \mathbf{A} & \mathbf{P} \\ \mathbf{P}^T & \mathbf{0} \end{bmatrix} \in \mathbb{R}^{(\mathbf{N+4})\times(\mathbf{N+4})}, \tag{2.17}$$

$$\mathbf{A} = \begin{bmatrix} \varphi_1(\mathbf{x}_1) & \cdots & \varphi_N(\mathbf{x}_1) \\ \vdots & \ddots & \vdots \\ \varphi_1(\mathbf{x}_N) & \cdots & \varphi_N(\mathbf{x}_N) \end{bmatrix} \in \mathbb{R}^{N\times N}, \tag{2.18}$$

$$\mathbf{P} = \begin{bmatrix} 1 & x_1 & y_1 & z_1 \\ \vdots & \vdots & \vdots & \vdots \\ 1 & x_N & y_N & z_N \end{bmatrix} \in \mathbb{R}^{N\times 4}, \tag{2.19}$$

$$\alpha = [\alpha_1 \ \cdots \ \alpha_N \, p_0 \, p_1 \, p_2 \, p_3 \,]^T \ \in \mathbb{R}^N, \tag{2.20}$$

and,

$$\mathbf{f} = [f_1 \ \cdots \ f_N \, 0 \, 0 \, 0 \, 0 \,]^T \ \in \mathbb{R}^N. \tag{2.21}$$

Since the collocation matrix $\mathbf{H}$ is theoretically invertible [33] [34] [35], the generalized expansion coefficients α can be given by:

$$\alpha = \mathbf{H}^{-1}\mathbf{f} \tag{2.22}$$

LU factorization or iterative means can be used to to solve the Equation 2.16 for relatively simple and small problems. However, these methods could become very computationally expensive and even impractical [36] when large or three-dimensional problems are applied. Therefore, rapid evaluation methods, based on the fast multipole method (FMM), which reduces storage and computational cost should be adopted. After obtaining the generalized coefficients of expansion α, the RBF interpolant resulting from the function implicit in Equation 2.12 can be compactly rewritten as:

$$\Phi(\mathbf{x}) = \boldsymbol{\phi}^T(\mathbf{x}\alpha), \tag{2.23}$$

where:

$$\boldsymbol{\phi}^T(\mathbf{x}) = [\varphi_1(\mathbf{x}) \ \cdots \ \varphi_N(\mathbf{x}) \ 1 \ x \ y \ z]^T \in \mathbb{R}^{(N+4)\times 1}. \tag{2.24}$$

2.4 Topology Optimization Based On Parameterized Level Set Optimization Method

This method consists of transforming the Hamilton Jacobi partial differential equation into a system of first-order ordinary differential equations ODEs over the entire D domain to solve topological optimization problems using the level set method efficiently with significant mathematical convenience. In topological optimization methods based on the traditional level set method, the edge of the shape is moved along the offset gradient direction to find an optimal shape and topology, this is equivalent to carrying the implicit scalar function $\mathbf{\Phi}(\mathbf{x})$ solving the Hamilton Jacobi-type Equation 2.9 and then the optimal front propagation is developed by solving the PDE Hamilton Jacobi 2.14. In the topological optimization method based on a parameterized level set, implicit modeling is used by means of RBF functions to interpolate $\mathbf{\Phi}(\mathbf{x})$ with N knots when using N radial-based multi-quadratic functions centered on these nodes. Because the Hamilton-Jacobi Equation 2.9 is time dependent, it is assumed that space and time are separable and the time dependence of the implicit function $\mathbf{\Phi}$ α of the RBF interpolate in Equation 2.20. With these assumptions, the RBF interpolant of the implicit function in Equation 2.23 becomes time dependent as follows:

$$\Phi = \Phi(\mathbf{x}, t) = \Phi^T(\mathbf{x})\alpha(t) \tag{2.25}$$

And the orthogonality constraints in Equation 2.14 can be rewritten like this:

$$\sum_{i=1}^{N} \alpha_i(t) = 0; \sum_{i=1}^{N} \alpha_i(t) x_i = 0; \sum_{i=1}^{N} \alpha_i(t) y_i = 0; \sum_{i=1}^{N} \alpha_i(t) z_i = 0; \tag{2.26}$$

Substituting Equation 2.25 into the Hamilton-Jacobi Equation 2.9 produces:

$$\Phi^T \frac{d\boldsymbol{\alpha}}{dt} + v_n \left| (\nabla \boldsymbol{\phi})^T \boldsymbol{\alpha} \right| = 0 \tag{2.27}$$

where:

$$\nabla\boldsymbol{\phi} = \frac{\partial\boldsymbol{\phi}}{\partial x}\mathbf{i} + \frac{\partial\boldsymbol{\phi}}{\partial y}\mathbf{j} + \frac{\partial\boldsymbol{\phi}}{\partial z}\mathbf{k} \tag{2.28}$$

$$\left|(\nabla\boldsymbol{\phi})^T\boldsymbol{\alpha}\right| = \left[(\tfrac{\partial\phi^T}{\partial x}\boldsymbol{\alpha})^2 + (\tfrac{\partial\phi^T}{\partial y}\boldsymbol{\alpha})^2 + (\tfrac{\partial\phi^T}{\partial z}\boldsymbol{\alpha})^2\right] \tag{2.29}$$

In Equation 2.27, the generalized coefficients of expansion are explicitly dependent on time and all dependence on time is due to them. In the initial time, all time-dependent variables should be specified over the entire design domain. This initial value problem can be considered equivalent to an interpolation problem since the coefficients of expansion in the initial time are found as the solution of an interpolation problem. As a consequence the original time-dependent problem has been converted into an interpolation problem for initial values of the generalized coefficients of expansion. $\boldsymbol{\alpha}$. To evolve in time the initial values of $\boldsymbol{\alpha}$, a method of placement is employed. This method describes a Eulerian-type approach, all the nodes of the fixed mesh are taken as the nodes of the RBF interpolation for the implicit function $\boldsymbol{\Phi}(\mathbf{x})$. As an extension, Equation 2.27 is then applied to each of the nodes of the RBF interpolation, rather than just to the points in front. Normal speed v_n in Equation 2.27 it is extended to v_n^e for all knots in the design domain D. This is illustrated in Figure 2.4, where each point of the grid is considered as a node of the RBF.

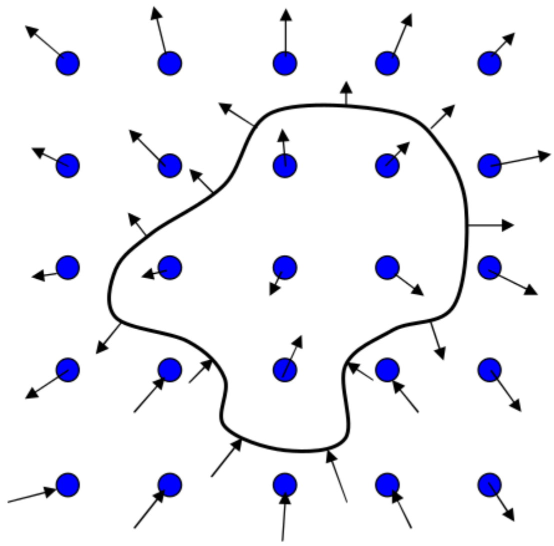

Figure 2.4: An extension velocity field for the parameterized level set method. Source: [2]

By using a method of placing the orthogonality constraints in Equation 2.26, a set of ODEs can be obtained like this:

$$\mathbf{H}\frac{d\boldsymbol{\alpha}}{dt} + \mathbf{B}(\boldsymbol{\alpha}) = 0 \tag{2.30}$$

where

$$\begin{bmatrix} v_n^e(\mathbf{x}_1)\left|(\nabla\boldsymbol{\phi}^T(\mathbf{x}_1))\boldsymbol{\alpha}\right| \\ \vdots \\ v_n^e(\mathbf{x}_N)\left|(\nabla\boldsymbol{\phi}^T(\mathbf{x}_N))\boldsymbol{\alpha}\right| \\ 0 \\ 0 \\ 0 \\ 0 \end{bmatrix} \in \mathbb{R}^{(N+4)\times 1} \tag{2.31}$$

It should be noted that Equation 2.30 is a collocation formulation of the lines method, in which a PDE problem is reduced to a simpler ODE problem by discretization. The method of lines has solid mathematical foundations and the convergence of the solution of the ODE problem converted to the solution of the original PDE problem has been rigorously tested. In Equation 2.31, the space derivative $\nabla\boldsymbol{\phi}$ can be calculated analytically from Equation 2.24 due to RBF interpolation.

The set of coupled nonlinear ODEs of Equation 2.30 can be solved by many ODE solvers such as first order forward Euler and the higher order Runge-Kutta. The present work uses the first order forward Euler method due to the simplicity of the algorithm. Euler algorithm can provide an approximate solution to Equation 2.30 which is given by:

$$\boldsymbol{\alpha}(t^{n+1}) = \boldsymbol{\alpha}(t^n) - \tau\mathbf{H}^{-1}\mathbf{B}(\boldsymbol{\alpha}(t^n)) \tag{2.32}$$

where τ is the step size. It should be noted that the step size must be small enough to achieve numerical stability due to the Courant-Friedrichs-Lewy condition (CFL) and to reduce truncation error due to the variation in each step of descent gradient direction and velocity field in Equation 2.27, in topological optimization methods based on the level set method. After obtaining an approximate solution to the equation 2.32 at each time step, the time-dependent shape and topology can be updated using the equation 2.25.

In topology and shape optimization methods based on level set methods, a reset procedure is required to recover the signed distance function behavior of the level set function. $\boldsymbol{\Phi}(\mathbf{x})$ in the vicinity of the front to ensure a good approximation of the normal or curvature to the front. However, the reset error is prone to accumulate as the number of time steps increases. Therefore, rebooting should be avoided as much as possible. Resetting produces a severe problem, which is that new holes cannot be created within a maetial region.

The topology and shape optimization method based on the parameterized level set method is capable of nucleation of holes and of eliminating the dependency of the final optimizes solution in the initial design.

Extension Velocity Method

In Eulerian approaches the normal velocity $v_n(\mathbf{x})$ the front must be extended and in the method of lines used in this work the normal speed $v_n^e(\mathbf{x})$ has the form shown in Equation 2.31 is the extension speed, which is defined over the entire design domain thus $v_N^e(\mathbf{x}) : D \to \mathbb{R}$. The choice of the extension speed method is crucial as it has a direct influence on the overall efficiency of the entire parameterized level set method 48. To ensure accurate and efficient time advance, the extension speed $v_n^e(\mathbf{x})$ it must be defined carefully.

There are many approaches to building extension speed $v_n^e(\mathbf{x})$. The original level set method introduced by Osher and Sethian [15] was focused on interface problems with geometric propagation velocities so that a natural construction of an extension velocity could be obtained, in which a signed distance function such as a level function due to its simplicity.

When there is no physically significant alternative, some researchers suggest constructing the extension velocity by extrapolating the velocity of front 70, which will require the location of the closest point on the grid.

In the method presented in this work, a physically significant extension rate method is used for topological optimization based on the implicit level set function. According to equation 5, a natural extension of a normal velocity can be obtained if the stress field is defined over the entire design domain D by assuming $\boldsymbol{\varepsilon}(\mathbf{u}) = 0$, $\mathbf{u} \in (D \setminus \Omega)$. Since the tension energy within the design domain and the Lagrange multiplier related to the volume constraint are included, this rate of extension is physically significant.

However, this extension introduces a discontinuity in velocity near the front because the stress field on is continuous along the front. To ensure a smooth front process, this discotinuity must be eliminated. The front itself is smooth and continuously differentiable due to the implicit RBF 53 modeling, but the magnitude of the normal velocity to the front might not be continuous or smooth enough due to the finite element modeling involved in stress analysis. Therefore, the magnitude of the normal velocity along the front must be smooth to allow stable propagation along the direction of gradient descent. To develop all these options, the front must be explicitly captured.

In the field of level set methods, it is well known that one of the most notable characteristics of the methods of this family is that the front does not need to be explicitly constructed and that the entire method can be developed on the underlying mesh. In order to make use of this feature, all smoothing operations are performed in a narrow band region, rather than just along the front. A narrow band region around the zero contour curve is defined as $\boldsymbol{\Xi} = \left\{ \mathbf{x} \in \mathbb{R}^d \mid \|\boldsymbol{\Phi}(\mathbf{x}) \leq \delta\| \right\}$, where δ is the width of the band. The speed of extension in the narrow band is still smoothed, thus using a simple linear filter (radially linear kernel hat) to achieve a good smoothing effect, which can be written as:

$$\widehat{v_n^e}(\mathbf{x}) = k^{-1}(\mathbf{x}) \sum_{\mathbf{p} \in N(\mathbf{x})} W_c(\|\mathbf{p} - \mathbf{x}\|) v_n^e(\mathbf{x}) \tag{2.33}$$

where:

$$k(\mathbf{x}) = \sum_{\mathbf{p} \in N(\mathbf{x})} W(\|\mathbf{p} - \mathbf{x}\|) \tag{2.34}$$

$$W(\|\mathbf{p} - \mathbf{x}\|) = r_{min} - \|\mathbf{p} - \mathbf{x}\| \tag{2.35}$$

in which $N(\mathbf{x})$ is the neighborhood of $\mathbf{x} \in \Xi$ in the filter window and r_{min} is the size of the window.

Therefore, the general extension speed is obtained as:

$$v_n^e(\mathbf{x}) = \begin{cases} (\boldsymbol{\varepsilon}(\mathbf{u}))^T \mathbf{C} \boldsymbol{\varepsilon}(\mathbf{u}) - l & \forall \mathbf{x} \in \mathbb{R}^d \, |\Phi(\mathbf{x}) < -\delta \\ \widehat{v_n^e}(\mathbf{x}) & \forall \mathbf{x} \in \Xi \\ -l & \forall \mathbf{x} \in \mathbb{R}^d \, |\Phi(\mathbf{x}) > \delta \end{cases} \tag{2.36}$$

It can be noted that the extension speed field used to move the level set function is related to the normal speed suggested by physics throughout the design domain and so the extension speed conveys information about the physics.

Due to the implicit RBF modeling and linear smoothing effect, the smoothness of the implicit level set function can be well maintained throughout the time advance without resetting.

Chapter 3

State of the Art

Topology optimization based on the traditional level set method was firstly proposed by Wang *et al.* in their work A level set method for structural topology optimization in 2003 [37]. Wang *et al.* described an approach to structural topology optimization that benefits from the flexible handling of complex topological changes and a concise description of the boundary shape features of the level set method. This approach describes a structural optimization procedure as a sequence of motions of the boundaries. The result is a 3D optimization method capable of handling topological changes and fidelity of boundary representation.

Wang *et al.* method [37] presents relevant drawbacks that limit its performance as the need for a reinitialization procedure and the lack of holes nucleation. Newer methods based on the Wang *et al.* approach overcome these drawbacks by implementing different mathematical tools like parameterization of the level set function as described in the work of Wang *et al.* [38]. This approach parameterizes the level set function using radial basis functions (RBF) and converts a PDE problem into a more mathematically convenient ODEs problem. This conversion alleviates the need for a complete reinitialization scheme and also allows holes nucleation. Thus, improving the performance and avoiding getting stuck in a local minimum.

Since the work of Wang *et al.* [38], topology optimization based on parameterized level set method has received significant interest in recent years. There were developed multiple methods to improve the optimization operation besides integrations with other fields, as mechanical engineering and machine learning.

3.1 Integration with Deep Learning and Additive Manufacturing

In the framework of topology optimization based on parameterized level set method, there were proposed deep learning-based parameterized level set methods to achieve topology optimization [3]. This method incorporates deep neural networks into the level set-based topology optimization method where the implicit function is described by a deep neural network. This approach guarantees smoothness and continuity of implicit function. Nowadays, most topology optimization methods find an optimal material layout that can maximize or minimize the objective function. Nevertheless, in real-world applications, diverse and competitive enough solutions can be required to make a choice based on functional or aesthetic requirements. Wang *et al.* [39] presented diverse and competitive designs by implementing a SIMP based-method with graphic diversity constraints. However, for parameterized level set methods, rare works are found in this field. Deng and To [3] proposed a DNN-based level set method to effectively generate diverse and competitive designs with high structural performance. Deng and To [3] describes a parametric level set method for topology optimization based on Deep Neural Network. Their proposal incorporates a fully connected deep neural network into the conventional level set method where the Hamilton-Jacobi partial differential equations PDEs are transformed into a parameterized ordinary differential equations ODEs. This approach of parameterization follows a similar schema to the present in this work, a PDE decoupled into a system of ODEs. The implicit function is updated by updating the network parameters. This method needs a reinitialization to prevent the implicit function to lose its signed distance function feature near the interface. The major feature of this method is its ability to generate diverse designs with different network architectures. This method represents an opportunity for a family of methods based on machine learning and topology optimization.

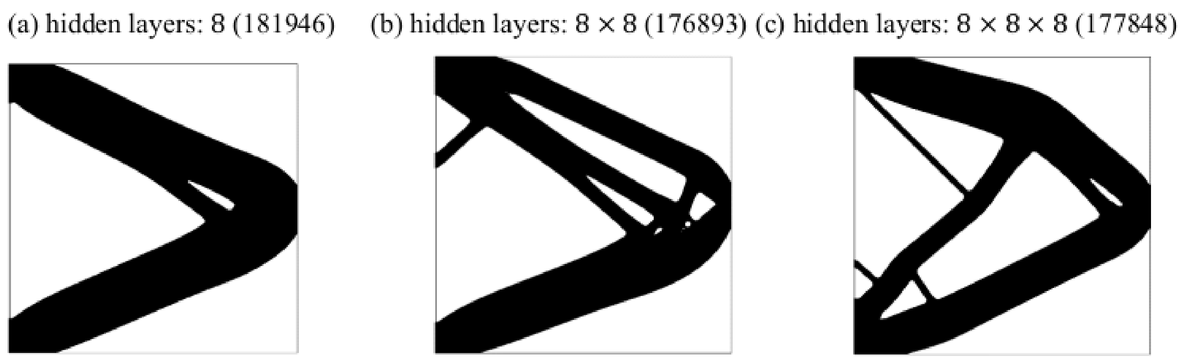

Figure 3.1: Diverse and competitive designs generated by DNN-based level set method. a) Desgined using 8 hidden layers, with a compliance of 181946. b) Desgined using 8×8 hidden layers, with a compliance of 176893. c) Desgined using $8 \times 8 \times 8$ hidden layers, with a compliance of 177848. Source: [3]

Topology optimization can be combined with manufacturing techniques to generate lightweight and high-performance structures that can be hard or even impossible to obtain through conventional methods. Additive manufacturing is an advanced manufacturing technique that, integrated with topology optimization, is capable of generating high-performance and complex structures. Zhu *et al.* [40] describe use cases of topology optimization integrated with additive manufacturing (AM) as the development of an antenna bracket for RUAG's sentinel satellite. This component exceeded maximum rigidity requirements by more than 30% and weight reduction from 1.6 kg. to 940 g.

It is shown that in the research of topology optimization for additive manufacturing, the integration of material, structure, process, and performance is important to pursue high-performance, multi-functional and lightweight production. Deng and To [3] describe

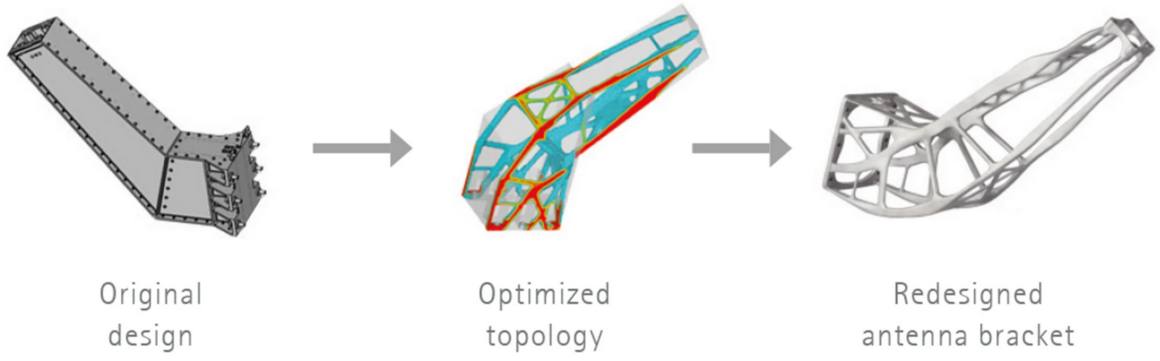

Figure 3.2: Antenna bracket for RUAG's sentinel satellite. Source: [4]

a parametric level set method for topology optimization based on Deep Neural Network. Their proposal incorporates a fully connected deep neural network into the conventional level set method where the Hamilton-Jacobi partial differential equations PDEs are transformed into a parameterized ordinary differential equations ODEs. This approach of parameterization follows a similar schema to the present in this work, a PDE decoupled into a system of ODEs. The implicit function is updated by updating the network parameters. This method needs a reinitialization to prevent the implicit function to lose its signed distance function feature near the interface. The major feature of this method is its ability to generate diverse designs with different network architectures. This method represents an opportunity for a family of methods based on machine learning and topology optimization.

In recent years, machine learning has received wide interest in applications to solve physical problems. The application of machine learning for physical problems is based on the capability to solve partial differential equations [41], [42], [43],[44]. In these approaches, physics-informed neural networks are trained to solve physical problems constrained by the laws of physics. The research of multiple machine learning-based approaches has led to developing methods to resolve topology optimization problems. Yu *et al.* [45] proposed a novel deep learning-based non-iterative method to predict optimal design with given boundary conditions. Lei *et al.* [46] proposed a machine learning-based method to perform real-time structural topology optimization. neural networks are trained to solve physical problems constrained by the laws of physics. The development of multiple machine learning-based approaches has led to research methods to resolve topology optimization problems. Yu *et al.* [45] proposed a novel deep learning-based non-iterative method to predict optimal design with given boundary conditions.

RBFs [33] have received much attention for the solution of structural optimization problems in the framework of parameterized level set method. The initial implementation was proposed by Wang and Wang [37], and further explored by Wang *et al.* [47] for efficiency and performance. The natural velocity extension in the implementation of RBFs in the level set method allows hole nucleation without the need for topological derivatives. Thus, alleviating the dependency on the initial design.

3.2 Advances in Topology Optimization improvements Based on the Parameterized Level Set Method

RBFs can be implemented in terms of global, local, and compactly supported domains. These different implementations have been studied for Siraj-ul-Islam *et al.* in their use in structural topology optimization [48]. In this work, it is highlighted the use of local radial basis functions LRBFs due to geometric and algebraic advantages that it offers.

The first approaches of parameterized level set function were developed using Global Radial Basis Functions GRBFs. Sarler presented a GRBFs-based Level Set Method (GRBFS-LSM) for structural topology optimization [49]. This study transformed the original Hamilton-Jacobi equation into a set of ODEs following the method of lines. The contributions reported in [50], have pinpointed a new field of application for the RBFs (in the case of global and compactly supported RBFs) in the structural optimization. One of the main disadvantages of the GRBFs is that the system matrix is notoriously ill-conditioned due to its strong dependence on the shape parameter value

Compactly supported Radial Basis Functions CS-RBF are strongly dependent on the appropriate support radius of the function. As a result, CS-RBFs are not suitable for data points that are further apart from the support radius and also if the data points are far closer to each other. CS-RBFs have a slow convergence rate and it is difficult to achieve convergence in large-scale interpolation problems [51]. The coefficient matrix is sparse and strictly positive definite.

Siraj-ul-Islam et al. in his work The localized radial basis functions for parameterized level set based structural optimization [5] explored the advantages in terms of convergence, stability, sensitivity, mesh dependency, and computational efficiency for the use of Locally Supported Radial Basis Functions LRBFs and its comparison with Globally Supported Radial Basis Functions GRBFs and Compactly Supported Radial Basis Functions CS-RBFs. These LRBFs have been applied with the level set method to structural applied shape and topology optimization for compliant mechanism problems [52].

Siraj-ul-Islam et al. presented an LRBFs based LSM (LRBFs-LSM) for minimum compliance of two-dimensional structural optimization problems. In their approach, the strain energy density field is obtained by the finite element method (FEM) using the ersatz material technique [53]. The geometry is represented with the LRBFs.

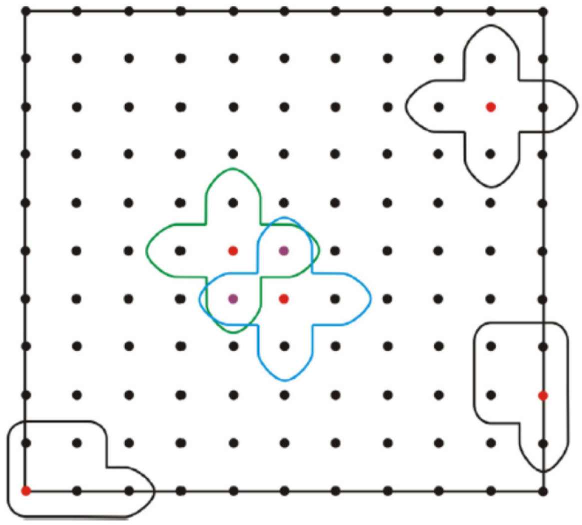

Figure 3.3: Schematic diagram of local support domain with 5 points stencil. Source: [5]

The conventional Hamilton-Jacobi equation is transformed into a system of ODEs. An approximate re-initialization is used [54, 55] during the evolution process. Due to the local support domain, the LRBFs-LSM requires less memory storage as compared to the GRBFs-LSM, which has a full dense matrix representation. In addition, the LRBFs-LSM is an efficient localized version of the GRBFs-LSM, which avoids breakdown during propagation and unstable solution [54]. Since the system matrix of the GRBFs-LSM is notoriously ill-conditioned due to its strong dependence on the shape parameter value, therefore, LRBFs, which produces a well-conditioned system matrix of the size of the local subdomain, within the LSM framework. In addition, the numerical tests performed suggest that due to the one-time inversion of a small collocation matrix, the LRBFs based collocation method is computationally more efficient. It has been also observed that the final solution obtained through LRBFs-LSM is comparatively less mesh and shape parameter-dependent, which is an important aspect of the implementation of LRBFs in the present work.

Chapter 4

Methodology

4.1 Phases of Problem Solving

4.1.1 Description of the Problem

An algorithm intended to solve an topology optimization problem, has to perform optimization and simulation procedures. The algorithm has to combine one first step of solving a system of coupled ODEs and a second step of finite elements that evolve over time.

Topological optimization is the process by which an object achieves the best arrangement of its components according to some criteria. In this work, compliance minimization is studied, which means minimizing the displacements of the material components caused by external forces. Then the topological optimization following the criterion of minimization of compliance, configures a body in such a way that the material of which it is composed is distributed in such a way that surpluses are eliminated that do not contribute to the rigidity of the body.

There are different approaches to performing this procedure, one of the most popular being the SIMP approach. For this work, the parameterized level set method was studied. This method arises as an improvement to the traditional level set method. Which was featured by Osher [15]. As already explained in Chapter 2 of this work, the level set method was developed as a method to follow the moving edge of an interface. This method, however, presented several drawbacks when used for topological optimization. Being, mainly, the difficulty and the numerical instability that causes to solve a partial differential equation and the incapacity of nucleation of new holes within the design domain. This can cause the optimization process to get stuck at a local minimum and an optimal topology is not achieved. Additionally, the traditional level set method is obliged to employ a reinitialization scheme to maintain the signed distance function characteristic of the phi function, this introduces more numerical errors and increases the difficulty of implementation of the method.

The parameterized level set method is capable of generating new holes within the design domain so it can achieve a global optimum. Additionally, you do not need a complete reboot scheme. Instead, fuzzy reset schemes are implemented. This method was explained in greater depth in Chapter 2 of this work.

The parameterized level set method can be used to optimize the topology of a 3-dimensional body. To do this, a 4-dimensional isosurface must be defined and the zero isosurface of this surface will represent the contour of the 3-dimensional body. Subsequently, the topology optimization can be divided into two sections. The first being a function interpolation problem, in which the generalized expansion coefficients 0 are found. These coefficients are updated with each iteration of the optimization process. In order to update these coefficients, a finite element formulation must be included in order to simulate the object. This involves defining element stiffness matrices and other specific characteristics of the body and material.

Additionally, it is necessary to implement an indexing scheme for nodes, nodes and elements of the object. Thus, considering the dimensions and edge conditions prescribed for each case.

4.1.2 Analysis of the Problem

The implementation of a three-dimensional topological optimization algorithm using the parameterized level set method can be divided into three sections: initialization of the level set function as a signed distance function, finite element analysis and evolution of the level set function.

The first section, the initialization of the level set function as a signed distance function, involves all the operations necessary to generate the generalized expansion coefficients zero. This procedure requires the definition of the meshes, which must meet the CFL condition, define the coordinates and diameter of the initial holes in the design domain, initialize the level set function as a signed distance function, initialize the quadratic basis function, construct the interpolation matrix of radial basis functions and finally generate an interpolation of the function, thus obtaining the coefficients alpha zero.

The next section corresponds to finite element analysis. In this section the indexing schemes for nodes, degrees of freedom and elements are defined. Subsequently, using the previously generated indexes, the edge conditions are defined, these define the support points of the body, as well as the loads that it supports. This is defined by characterizing the degrees of freedom of each node as free or as fixed. Later in this section, properties of the object to be optimized must be defined. These properties are `E0` which represents represents the density of material in a filled section of the object. `Emin`, which represents the density of material in a section corresponding to a hole within the design domain. The Poisson's ratio `nu` which represents the elastic constant of the material. This coefficient is used to construct the element stiffness matrix KE. Since the material is considered homogeneous and isotropic, this `KE` matrix is the same for all the elements that make up the object. Subsequently, a connectivity matrix of the degrees of freedom must be built, this matrix is used to generate the x and y coordinates of a sparse matrix of the free degrees of freedom. Finally, the vectors of external forces and kinetically admissible motions F and U, respectively, must be constructed.

The last section of the algorithm implementation corresponds to the optimization loop. In this stage the following parameters are defined: maximum number of iterations allowed, number of iterations with relaxed volume restriction, the size of the time step, delta, mu and gamma which are parameters of the Lagrange multiplier. The light iteration begins by determining the elements of the object that are above the isosurface zero. This allows to calculate the volume of the object, which is constrained. The elements with a volume greater than zero are also needed to be able to calculate the vector `sK`, this vector together with the coordinates of the degrees of freedom x and y make up the dispersed matrix of global stiffness. This matrix is used to update the vector of kinetically admissible motions U. Subsequently, the fulfillment of each element of the object must be calculated, and by adding this vector, the global fulfillment of the object can be calculated. This optimization loop must also implement a convergence criterion. For the present work, the maximum number of iterations and the volume restriction must be considered. In this section, we also calculate the lagrange multiplier, which is related to the volume constraint. This multiplier is calculated differently during the first iterations corresponding to nRelax. Finally, the evolution of the level set function is carried out. Delta should be considered at this stage. Check. The deformation energy density of each element must also be mapped to its respective nodes in order to build the matrix `B`. This matrix, together with the interpolation matrix `G`, are used to update alpha by means of the Euler method to form first order. By obtaining the new generalized coefficients of expansion, the new function `phi` can be calculated.

4.1.3 Algorithm Design

The algorithm was designed following the scheme proposed by Wei [55]. In this proposal, the mesh, the signed distance function, is initialized first, and the first interpolation is performed using radial basis functions. Later the optimization loop starts. Within this loop, the strain energy density is calculated using finite element analysis. Using this result, the generalized expansion coefficients alpha are updated and finally the function `phi` is updated. As the last step, the convergence condition of the optimization loop is verified. The flowchart of the proposed method is illustrated in Figure 4.1

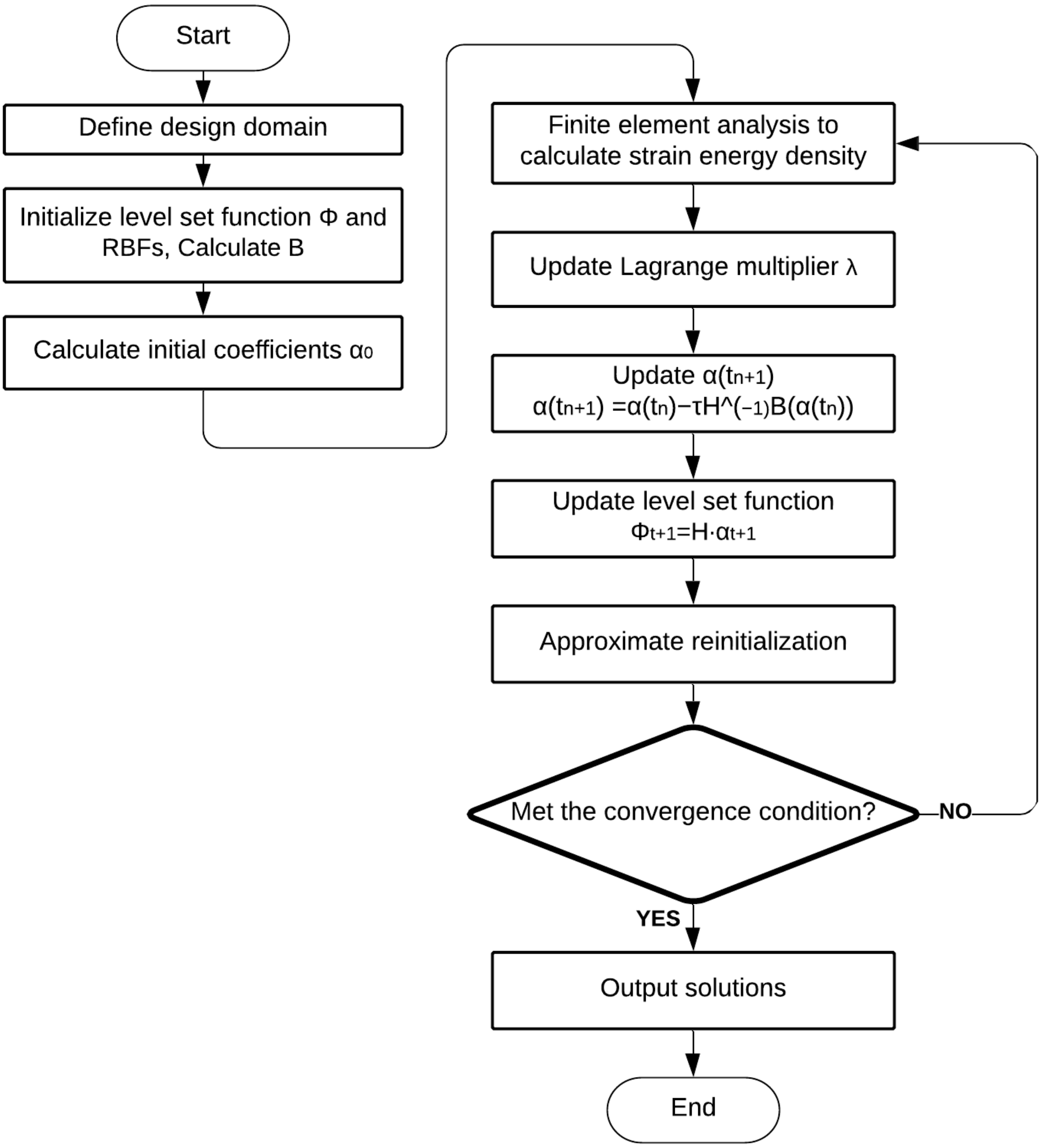

Figure 4.1: The flowchart of the proposed method

4.1.4 Implementation

The implementation was done using Matlab, without the use of external software packages and can be found in `https://github.com/eddyerach/top3dPLSM/tree/master`. The function to generate the element stiffness matrix `KE` was taken from the work of Liu and Tovar [6].

Algorithm implementation can be divided in five sections, there are: Level set function initialization, radial basis function initialization, finite element analysis preparation, boundary conditions definitions, iteration optimization.

The first section, level set function initialization has to define the initial holes coordinates and size. Position, number, and size of the initial holes have an impact on the time required to reach the optimum state. In this section there are also defined the grid according to the prescribed number of elements in x,y, and z dimension respectively, and the level set functions as a cube.

The second section, is aimed to perform a radial basis function interpolation over the level set function initialized in the first section. The radial basis function performed here has to compute the partial derivatives on the `X` and `Y` axis and the generalized expansion coefficients that will be used next to evolve the surface.

The third section, the finite element analysis preparation, has to define material properties like the Poisson coefficient. One of the most complex aspects of the implementation is to define an indexing schema for elements, nodes, and degrees of freedom. The approach used in this work is based on the work of Liu and Tovar [6]. This schema is explained in the Table 4.1.

Finite Elements Analysis

The body is discretized in a prismatic structure described in Figure 4.2 composed of eight eight-node cubic elements of the same size. The nodes identified with a numerical ID are ordered column-wise up-to-bottom, left-to-right, and back-to-front. The position of each node is defined with respect to the Cartesian coordinate system with origin at the left-bottom-back corner. The eight nodes $N_1, \cdots, N_8$ of each element is ordered in counterclockwise direction as shown in Figure 4.3. It is important to note that the local node number N_i does not follow the same rule as the global node ID system in Figure 4.2 Following the indexing approach and the size of the volume can be identified the global node coordinates and node IDs of the other seven nodes in the element by the mapping the relationships summarized in Table 4.1. As the problem deals with a three dimensional body, each node in it has three degrees of freedom (DOF) corresponding to linear displacements in x, y, and z directions. These degrees of freedom are stored in the nodal displacement vector `U` as:

$$\mathbf{U} = [U_{1x}, U_{1y}, U_{1z}, \cdots, U_{8\times nz}]^T, \tag{4.1}$$

Table 4.1: Illustration of relationships between node number, node coordinates, node ID and node DOFs

Node Number	**Node coordinates**	**Node ID**	**Node Degree of Freedoms**		
			x	**y**	**z**
N_1	(x_1, y_1, z_1)	NID_1	$3 \times NID_1 - 2$	$3 \times NID_1 - 1$	$3 \times NID_1$
N_2	$(x1+1, y1, z1)$	$NIID2 = NID1 + (nely+1)$	3 * NID2 - 2	$3 * NIDI2 - 1$	3 * NID2
N_3	$(x1+1, y1+1, z1)$	$NIID3 = NID1 + nely$	$3 * NID3 - 2$	$3 * NID3 - 1$	$3 * NID3$
N_4	$(x1, y1+1, z1)$	$NIID4 = NID1 - 1$	$3 * NID4 - 2$	$3 * NID4 - 1$	$3 * NID4$
N_5	$(x1, y, z1+1)$	$NIID5 = NID1 + NIDz$	$3 * NID5 - 2$	$3 * NID5 - 1$	$3 * NID5$
N_6	$(x1+1, y1, z1+1)$	$NIID6 = NID2 + NIDz$	$3 * NID6 - 2$	$3 * NID6 - 1$	$3 * NID6$
N_7	$(x1+1, y1+1, z1+1)$	$NIID7 = NID3 + NIDz$	$3 * NID7 - 2$	$3 * NID7 - 1$	$3 * NID7$
N_8	$(x1, y1+1, z1+1)$	$NIID8 = NID4 + NIDz$	$3 * NID8 - 2$	$3 * NID8 - 1$	$3 * NID8$

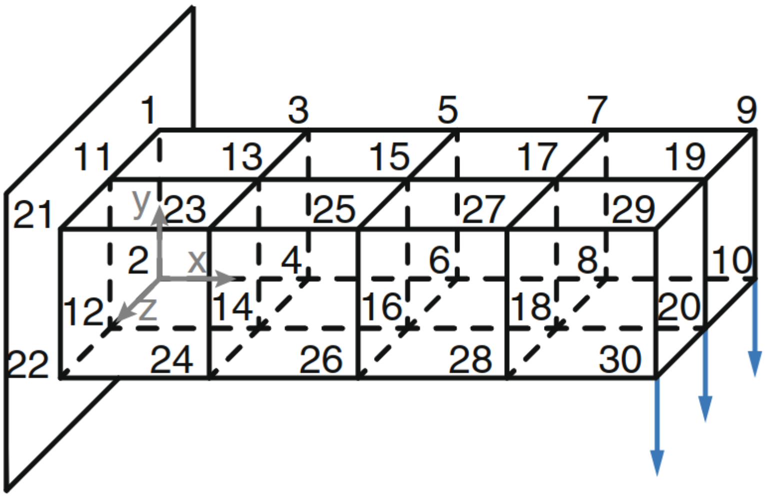

Figure 4.2: Node IDs global indexing scheme in a prismatic structure. Source: [6]

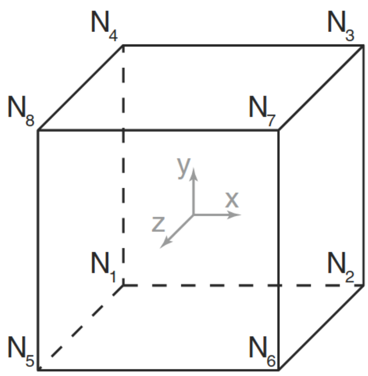

Figure 4.3: Node IDs local indexing scheme in a prismatic structure. Source: [6].

where n is the number of elements in the structure (`nelx` $\times$ `nely` $\times$ `nelz`). The organization of the DOFs in `U`, and consequently `K` and `F`, can be determined following the relationships described in Table. 4.1.

The node IDs for each element are located in a connectivity matrix `edofMat` with the following MATLAB lines:

```
function [cont] = auxiliar(nelx,nely,nelz)
cont = zeros(nelx*nely*nelz,8);
numElem = 1;
for z1 = 0:nelz-1
    for x1 = 0:nelx-1
        for y1 = nely-1:-1:0
            nidz = (nelx+1)*(nely+1);
            cont(numElem,4) = (z1*(nelx+1)*(nely+1))+(x1*(nely+1))+(
                nely+1-y1);
```

```
                cont(numElem,3) = cont(numElem,4) + (nely+1);
                cont(numElem,2) = cont(numElem,4) + nely;
                cont(numElem,1) = cont(numElem,4) - 1;
                cont(numElem,5) = cont(numElem,1) + nidz;
                cont(numElem,7) = cont(numElem,3) + nidz;
                cont(numElem,6) = cont(numElem,2) + nidz;
                cont(numElem,8) = cont(numElem,4) + nidz;
                numElem = numElem + 1;
            end
        end
    end
end
eleNode = auxiliar(nelx,nely,nelz);
edofMat = kron(eleNode,[3,3,3])+repmat([-2,-1,0],nelx*nely*nelz,8);
```

In the previous listing, `nele` is the number of elements in the structure, `nodegrd` contains the node ID of the first grid of nodes in the $x - y$ plane, for $z = 0$, the column vector `edofVec` contains the node IDs of the first node at each element, and the connectivity matrix `edofMat` of size `nele` $\times 24$ containing the node IDs for each element. For the volume in Figure 4.2, $\texttt{nelx} = 4, \texttt{nely} = 1$, and $\texttt{nelz} = 2$, which results in

$$edofMat = \begin{bmatrix} 1 & 2 & 3 & \cdots & 34 & 35 & 36 \\ 7 & 8 & 9 & \cdots & 40 & 41 & 42 \\ 13 & 14 & 15 & \cdots & 46 & 47 & 48 \\ 19 & 20 & 21 & \cdots & 52 & 53 & 54 \\ 31 & 32 & 33 & \cdots & 64 & 65 & 66 \\ 37 & 38 & 39 & \cdots & 70 & 71 & 72 \\ 43 & 44 & 45 & \cdots & 76 & 77 & 78 \\ 49 & 50 & 51 & \cdots & 82 & 83 & 84 \end{bmatrix} \tag{4.2}$$

The matrix `edofMat` is used to build the global stiffness matrix `K` as follows:

```
KE = lk_H8(nu);
eleNode = auxiliar(nelx,nely,nelz);
edofMat = kron(eleNode,[3,3,3])+repmat([-2,-1,0],nelx*nely*nelz,8);
iK = reshape(kron(edofMat,ones(24,1))',24*24*nelx*nely*nelz,1);
jK = reshape(kron(edofMat,ones(1,24))',24*24*nelx*nely*nelz,1);
sK = reshape(KE(:)*(Emin+eleVol'*(E0-Emin)),24*24*nelx*nely*nelz,1);
K = sparse(iK,jK,sK); K = (K+K')/2;
```

The matrix `KE` corresponding to the element stiffness matrix is generated from the lk_H8 subroutine that was taken from Liu and Tovar [6]. Matrices `iK` and `jK`, reshaped as column vectors, contain the coordinates of $24 \times 24 \times$ `nele` degrees of freedom in the structure. The matrix `sK` contains all element stiffness matrices. The building procedure of the matrix `K` avoids the use of nested for loops.

The nodal displacement vector `U` is obtained by solving the linear system formed by the stiffness matrix `K` and the vector of nodal forces `F`.

```
U(freedofs,1) = K(freedofs,freedofs)\F(freedofs,1);
eleComp = sum((U(edofMat)*KE).*U(edofMat),2).*(Emin+eleVol*(E0-Emin));
comp(iT) = sum(eleComp);
```

where the vector **freedofs** has the indices of the unconstrained DOFs. Subsequently, **U** is used to calculate the equivalent Young's modulus in the element stiffnes matrix. Finally, the velocities field or so called element strain energy field **eleComp** and the objective function value **comp** are calculated.

For the cantilevered structure in Figure 4.2, the constrained DOF

```
[jf,kf] = meshgrid(1:nely+1,1:nelz+1);                      % Coordinates*
fixednid = (kf-1)*(nely+1)*(nelx+1)+jf;                     % Node IDs*
fixeddofs = [3*fixednid(:); 3*fixednid(:)-1; 3*fixednid(:)-2]; % DOFs*
```

where **jf** and **kf** are the coordinates of the fixed nodes, **fixednid** are the node IDs that have displacement constraints, **fixeddof** are the location of the degrees of freedom that have displacement constraints also. The free degrees of freedom, are defined as

```
ndof = 3*(nelx+1)*(nely+1)*(nelz+1);%
freedofs = setdiff(1:ndof,fixeddofs);%
```

where **ndof** is the total number of degrees of freedom. The default configuration constraints the left face of the structure and assigns a vertical load to the structure's lower edge as shown in Figure 4.2. This configuration can be customized in order to produce different topology optimization scenarios.

4.1.5 Testing

The code is executed in Matlab with the following command:

```
top3dPLSM(nelx , nely , nelz , volfrac)
```

where **nelx**, **nely**, and **nelz** are the number of elements along x, y, and z directions. **volfrac** is the volume fraction constraint. The code is aimed to solve minimum compliance problems.

The software is highly customizable by the user, by allowing to configure material properties, number of elements in each direction, supports and loads, and PLSM topology optimization method parameters. This feature allow to simulate a wide variety of use case of topology optimization.

The following examples demonstrate the testing of the code to minimum compliance problems.

Short Cantilevered Beam

The configuration for this testing case are summarized in Tab. 4.2. These configurations establish a solid, elastic and isotropic prismatic structure. The supports and loads configuration are given by the following lines:

```
USER-DEFINED LOAD DOFs
il = nelx; jl = nely; kl = 0:nelz;                       % Coordinates*
loadnid = kl*(nelx+1)*(nely+1)+il*(nely+1)+(nely+1-jl); % Node IDs*
loaddof = 3*loadnid(:) - 1;                             % DOFs* termino fuente
% USER-DEFINED SUPPORT FIXED DOFs
[jf,kf] = meshgrid(1:nely+1,1:nelz+1);                  % Coordinates*
fixednid = (kf-1)*(nely+1)*(nelx+1)+jf;                 % Node IDs*
fixeddofs = [3*fixednid(:); 3*fixednid(:)-1; 3*fixednid(:)-2]; % DOFs*
```

where `il`, `jl`, and `kl` are the coordinates of the vertical load that is placed at the right face lower-edge. This load is applied to the whole edge. `loadnid` is the vector containing node ids that are directly affected by the load. `loaddof` holds the degrees of freedom of nodes beign directly affected by the load.

`jk`, and `kf` hold a mesh of coordinates of the supporting places. For this testing case, the supporting place is the whole left face of the structure. `fixednid` are the node ids for all nodes that belong to the supporting plane. `fixeddofs` are the degrees of freedom of the nodes in `fixednid`. These DOFs determine the kinematically admissible linear displacement and will remain fixed for all the optimization procedure.

Table 4.2: Experiment 1: Parameters configuration

Parameter	**Value**
`nelx`	12
`nely`	8
`nelz`	12
`volfrac`	0.3
`E0`	1
`Emin`	1e-9
`nu`	0.3
`dt`	0.01
`delta`	10
`mu`	20

4.2 Experimental Setup

4.2.1 Hardware

Table 4.3: Hardware Setup

Name	Description
CPU	AMD Ryzen 7 4800H, 8 Cores 16 Threads. Base Clock 2.9 Ghz
Memory	16 Gb DDR4
GPU	Nvidia GTX 1660 Ti Mobile

4.2.2 Software

Table 4.4: Software Setup

Name	Description
Operating System	Windows 10 Home 64-bits
MATLAB	R2019a (9.6.0.1072779) 64-bits

Chapter 5

Results and Discussion

5.1 Experiments, Results, and Discussion

The obtained results used the popular model "ersatz model" to calculate the strain energy of elements. The level set function is initially configured as a signed distance function with further approximated re-initializations. The RBF knots are assumed to be identical to the FEA nodes for the sake of simplicity. The multiquadric RBF is applied to all the numerical cases. The Young modulus of material is xGpa and Poisson's ratio is 0.3. In all cases, the design domains are discretized as eight-noded cube finite elements. All experiments were run with the same hardware and software configurations detailed in Section 4.4.

5.1.1 Experiment 1: Short Cantilevered Beam

In this experiment, it is studied the optimization problem of a short cantilever beam under single load. The design problem of the 3D structure is shown in Figure 4. The entire design domain is a cuboid solid with a dimension of 12×8×12 units. The left end is fixed and a vertical unit external force of magnitude 300kN is applied at the right-bottom end. The objective is to minimize the total strain energy of the structure for a given amount of material usage (30%). The configuration for this experiment is described in Table 4.2.

The optimization process iterated 160 times until it met the convergence condition as is shown in Figure 5.1. This condition is met when the volume and compliance do not exceed a difference threshold in the last 9 iterations. This difference is set to $1e^{-3}$ as for all experiments. The volume was constantly reduced in each iteration, going from the full volume of a solid cube to an optimized structure with 30% of the initial volume. As the volume was reduced, the compliance increased at the same rate, going from 300 to 780.

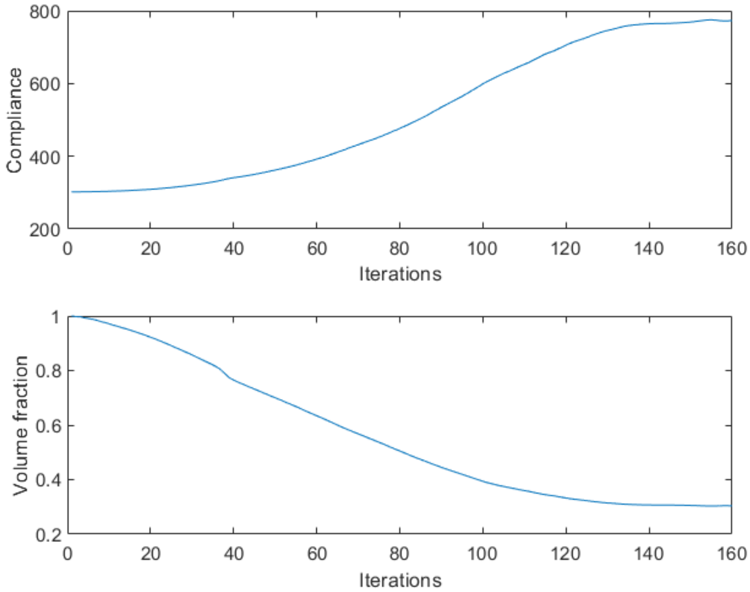

Figure 5.1: Experiment 1: Compliance and Volume *vs* Iterations. Object compliance increases as object volume decreases with each optimization iteration. This is due to the continuous reduction of the material, which decreases the stiffness of the body.

In the optimization process, the parameterization step involves the generation of generalized expansion coefficients α; these coefficients have to meet the constraints specified in the Eq. . The value of these constraints are tracked for each iteration to ensure that the RBF interpolation has the desired behavior as shown in Figure 5.2. There are 4 constraints that have to be equal to zero and in the experiments the value of the constraints ranged around zero. This oscillating behavior can be attributed to numerical errors.

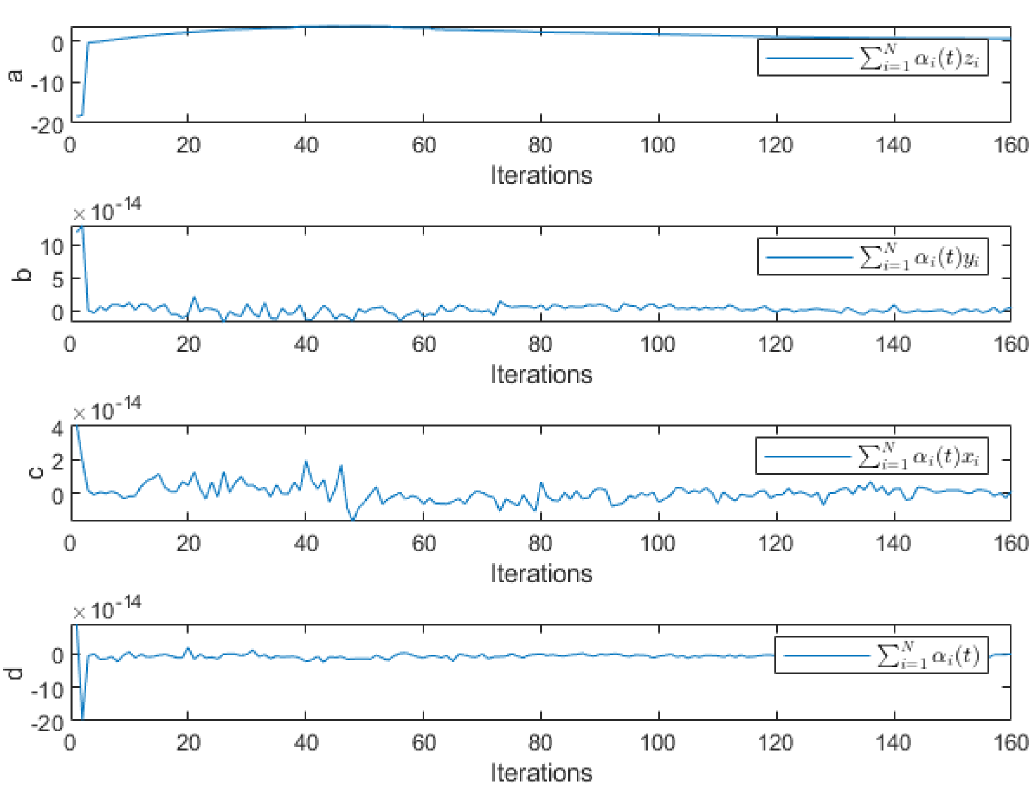

Figure 5.2: Experiment 1: Orthogonality constraints *vs* iterations. a, b, c, and d describes the time evolution of orthogonality constraints for z, x, y, and α_i values respectively. These restrictions are hold since they oscillate around zero which is the expected theoretical value.

The final result of this experiment shows a topologically optimal beam, supported by two segments at the left faces and holding the load at the full right-lower edge. This result is similar in appearance to the reported in literature. In Figure 5.3 can be seen the lower face of the structure, which has an interior hole, and two structural components connecting the lower support and the load. The side view can be seen in Figure 5.4, where is evident the optimal design aimed to reduce the compliance.

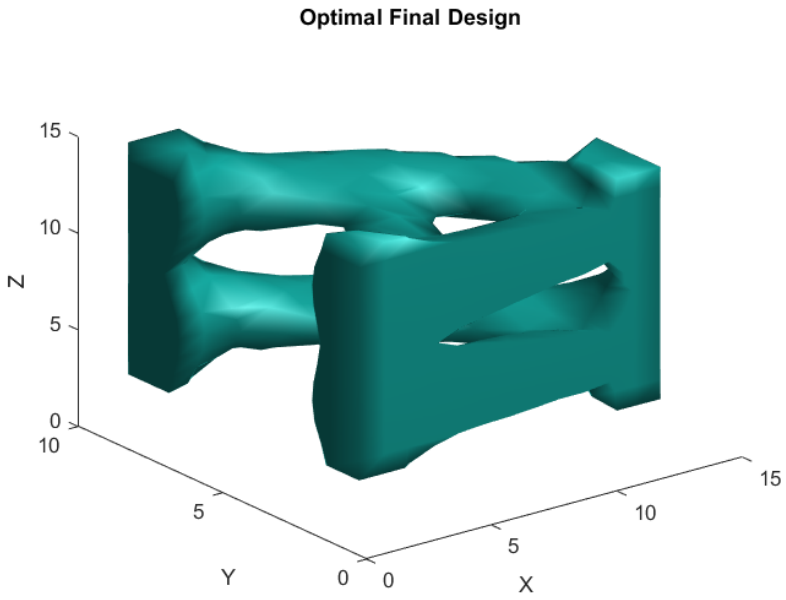

Figure 5.3: Experiment 1: Optimal topological design achieved when the convergence criterion is met.

Top perspective of the optimal design can be viewed in Figure 5.4. From this perspective can be appreciated the support elements at the left of the Figure, and the load at the lower right edge of the object. Also, can be appreciated a structure similar to the reported in literature.

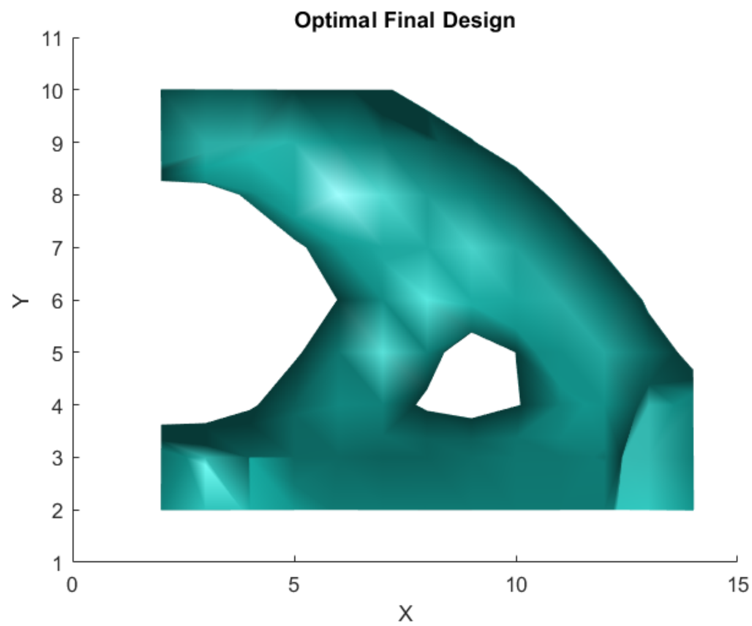

Figure 5.4: Experiment 1: Top view of optimized topological design. The agreement between the loads and supports and the design achieved is appreciated.

The three dimensional nature of the problems, generates tubular structures to achieve the minimum compliance. These features can be seen in Figure 5.5.

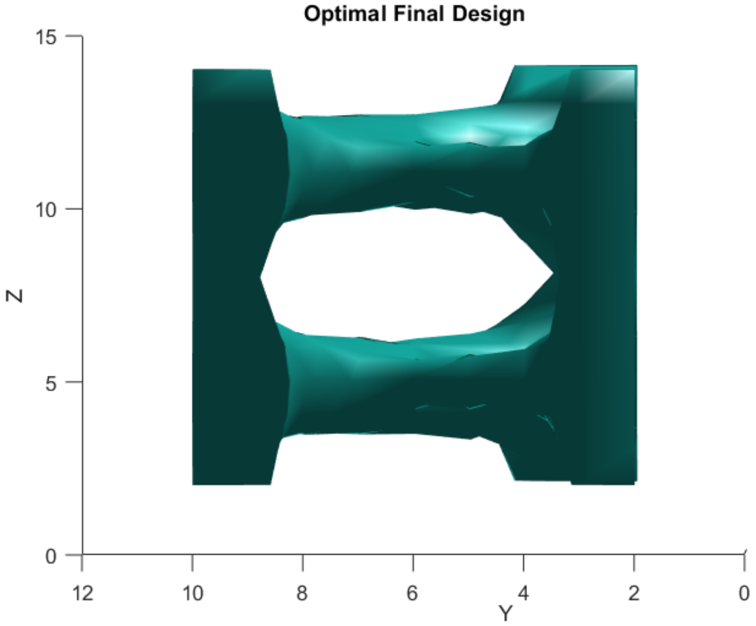

Figure 5.5: Experiment 1: Side perspective of the optimized topological design. The agreement between the loads and supports and the design achieved is appreciated. A symmetry in the structure of the body can also be evidenced, this due to supports and loads are defined throughout the length of the z axis.

5.1.2 Experiment 2: Cantilevered Beam

In this experiment, it is studied a variation of the Experiment 1: optimization problem of a cantilever beam under single load. The design problem of the 3D structure is the same as the first experiment. The entire design domain is a cuboid solid with $60 \times 20 \times 4$ units. The left end is fixed and a vertical unit external force of magnitude 300kN is applied at the right-bottom end. The objective is to minimize the total strain energy of the structure for a given amount of material usage (30%). The configuration for this experiment is described in Table 5.1.

The optimization process iterated 160 times until it met the convergence condition as is shown in Figure 5.11. The number of iterations needed to met the convergence condition was equal to the experiment 1. The volume was constantly reduced in each iteration, going from the full volume of a solid cube to an optimized structure with 30% of the initial volume. As the volume was reduced, the compliance increased at the same rate, going from 300 to 780.

Table 5.1: Experiment 2: Parameters configuration

Parameter	**Value**
`nelx`	60
`nely`	20
`nelz`	4
`volfrac`	0.3
`E0`	1
`Emin`	1e-9
`nu`	0.3
`dt`	0.01
`delta`	10
`mu`	20

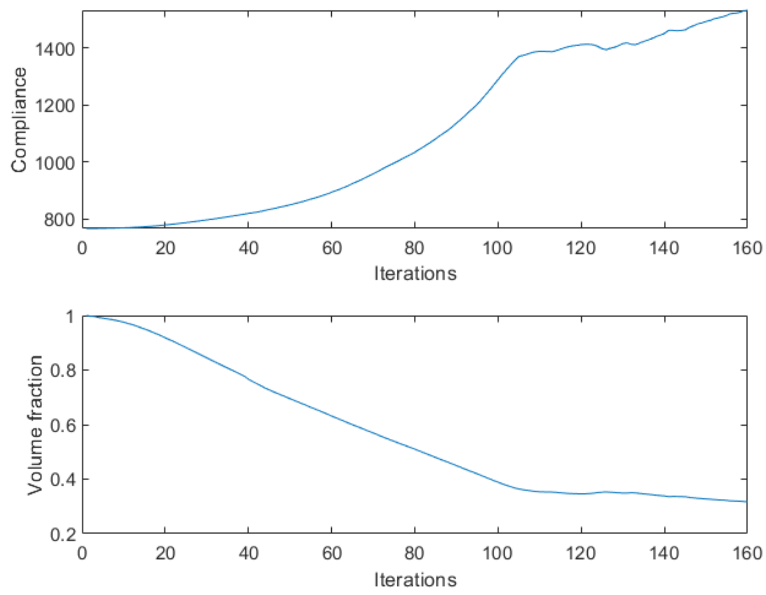

Figure 5.6: Experiment 2: Compliance and Volume *vs* Iterations. Object compliance increases as object volume decreases with each optimization iteration. This is due to the continuous reduction of the material, which decreases the stiffness of the body.

In the optimization process, the parameterization step involves the generation of generalized expansion coefficients α; these coefficients have to meet the constraints specified in the Equation . The value of these constraints are tracked for each iteration to ensure that the RBF interpolation has the desired behavior as shown in Figure 5.12. There are 4 constraints that have to be equal to zero and in the experiments the value of the constraints ranged around zero. This oscillating behavior can be attributed to numerical errors.

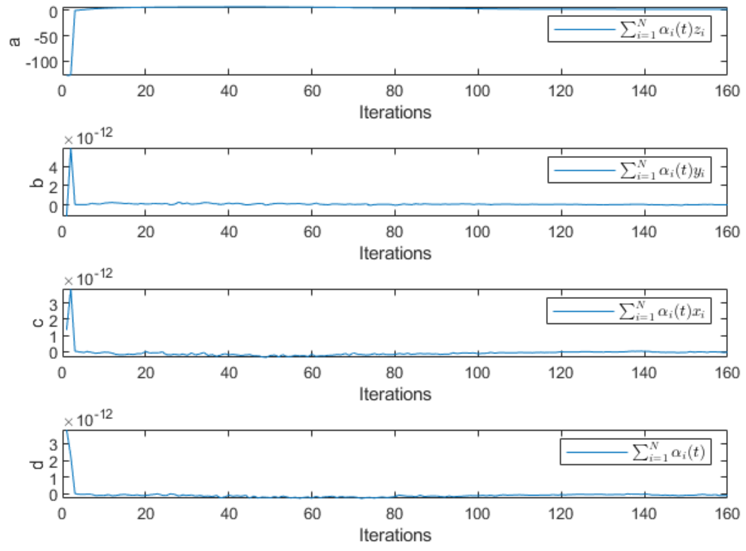

Figure 5.7: Experiment 2:Orthogonality constraints *vs* iterations. a, b, c, and d describes the time evolution of orthogonality constraints for z, x, y, and α_i values respectively. These restrictions are hold since they oscillate around zero which is the expected theoretical value

The final result of this experiment shows a topologically optimal beam, supported by two segments at the left faces and holding the load at the full right-lower edge. This result is similar in appearance to the reported in literature. In Figure 5.13 can be seen the lower face of the structure, which has an interior hole, and two structural components connecting the lower support and the load. The side view can be seen in Figure 5.9, where is evident the optimal design aimed to reduce the compliance.

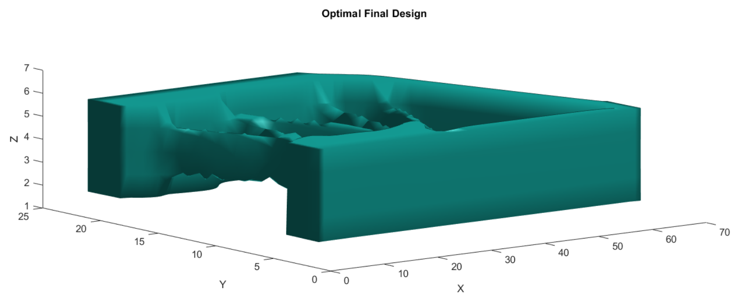

Figure 5.8: Experiment 2: Optimal topological design achieved when the convergence criterion is met.

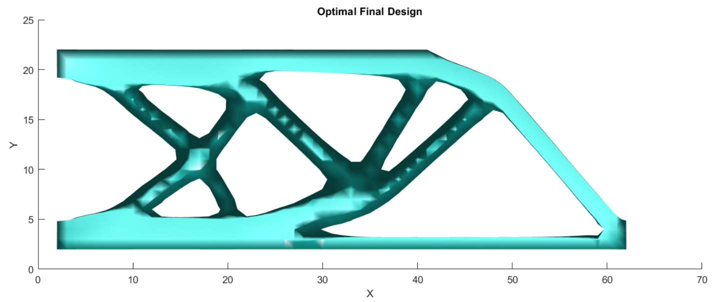

Figure 5.9: Experiment 2: Optimum topology from top perspective

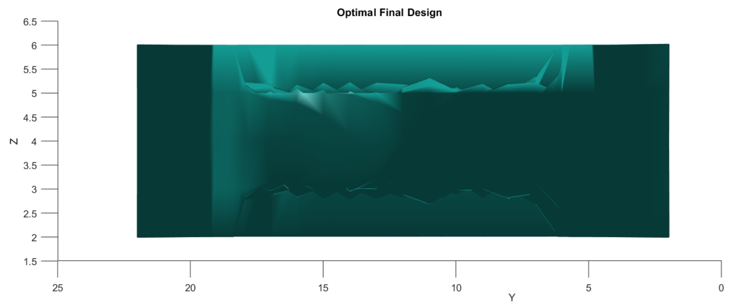

Figure 5.10: Experiment 2: Side perspective of the optimized topological design. The agreement between the loads and supports and the design achieved is appreciated. A symmetry in the structure of the body can also be evidenced, this due to supports and loads are defined throughout the length of the z axis.

5.1.3 Experiment 3: Short Beam, Single Load In The Middle

In this experiment, it is studied a variation of the past single loaded experiments, optimization problem of cantilever beam under single load in the middle of the right face. The design problem of the 3D structure is the same as the first experiments. The entire design domain follows the solid cuboid configuration shown in Table 5.2 with dimension of 24×16×8 units. The left end is fixed and a vertical unit external force of magnitude 300kN is applied at the right-middle end. The objective is to minimize the total strain energy of the structure for a given amount of material usage (30%). The optimization process iterated 160 times until it met the convergence condition as is shown in Figure 5.11. The number of iterations needed to met the convergence condition was equal to the other single load experiments. The volume was constantly reduced in each iteration, going from the full volume of a solid cube to an optimized structure with 30% of the initial volume. As the volume was reduced, the compliance increased at the same rate, going from 190 to 420

Table 5.2: Experiment 3: Parameters configuration

Parameter	**Value**
`nelx`	24
`nely`	16
`nelz`	8
`volfrac`	0.3
`E0`	1
`Emin`	1e-9
`nu`	0.3
`dt`	0.01
`delta`	10
`mu`	20

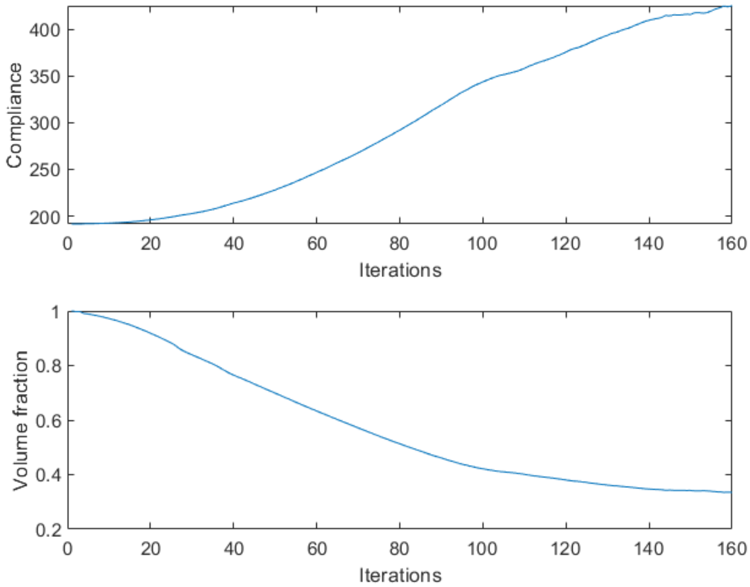

Figure 5.11: Experiment 3: Compliance and Volume *vs* Iterations. Object compliance increases as object volume decreases with each optimization iteration. This is due to the continuous reduction of the material, which decreases the stiffness of the body.

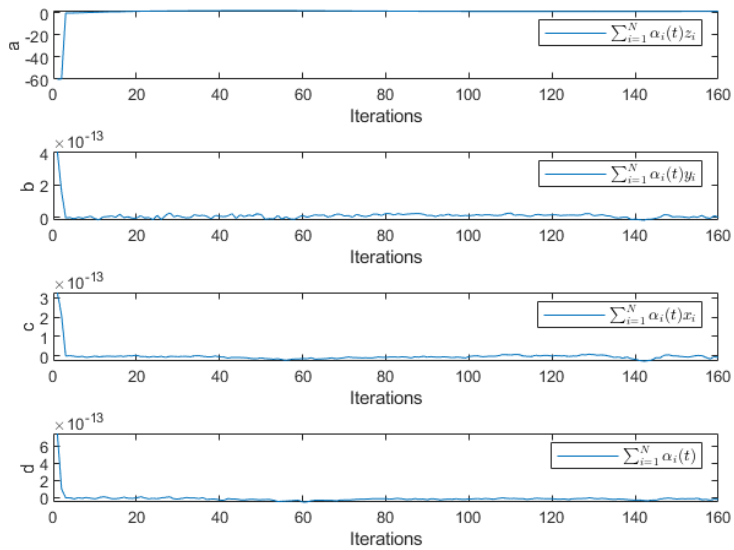

Figure 5.12: Experiment 3: Orthogonality constraints *vs* iterations. a, b, c, and d describes the time evolution of orthogonality constraints for z, x, y, and α_i values respectively. These restrictions are hold since they oscillate around zero which is the expected theoretical value

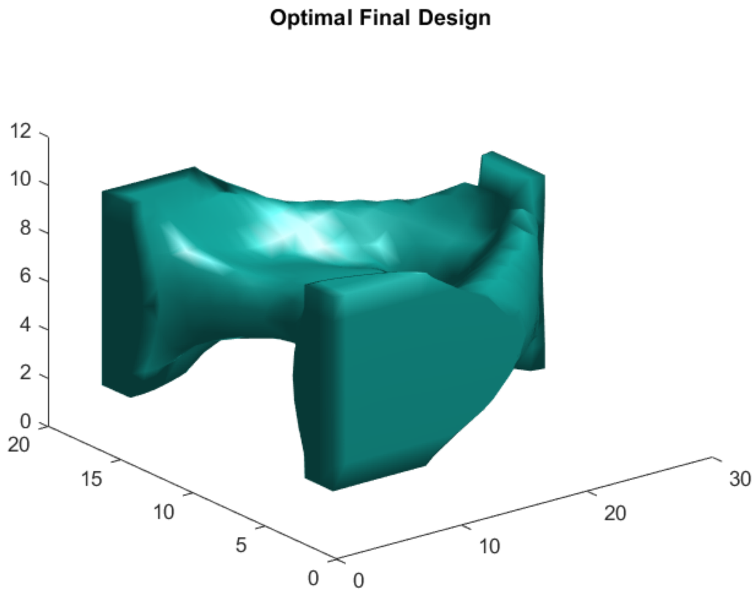

Figure 5.13: Experiment 3: Optimal topological design achieved when the convergence criterion is met.

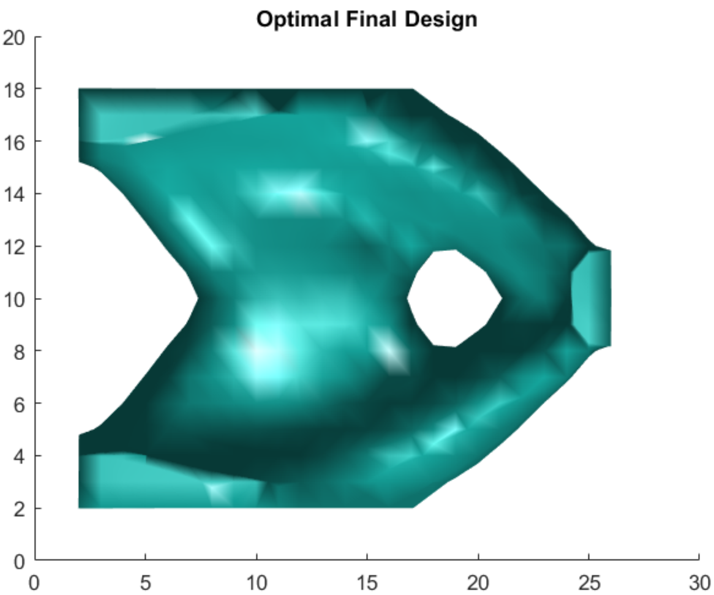

Figure 5.14: Experiment 3: Top view of optimized topological design. The agreement between the loads and supports and the design achieved is appreciated.

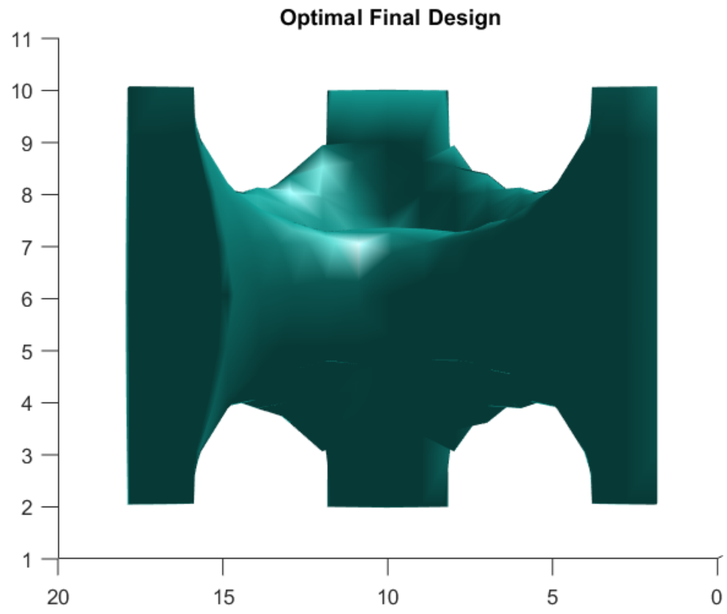

Figure 5.15: Experiment 3: Side perspective of the optimized topological design. The agreement between the loads and supports and the design achieved is appreciated. A symmetry in the structure of the body can also be evidenced, this due to supports and loads are defined throughout the length of the z axis.

5.2 Benchmarking

The results obtained were compared with published results from other authors. These results were obtained through variations of the parameterized level set method or through the SIMP method, as appropriate.

5.2.1 GRBFs-based PLSM vs SIMP

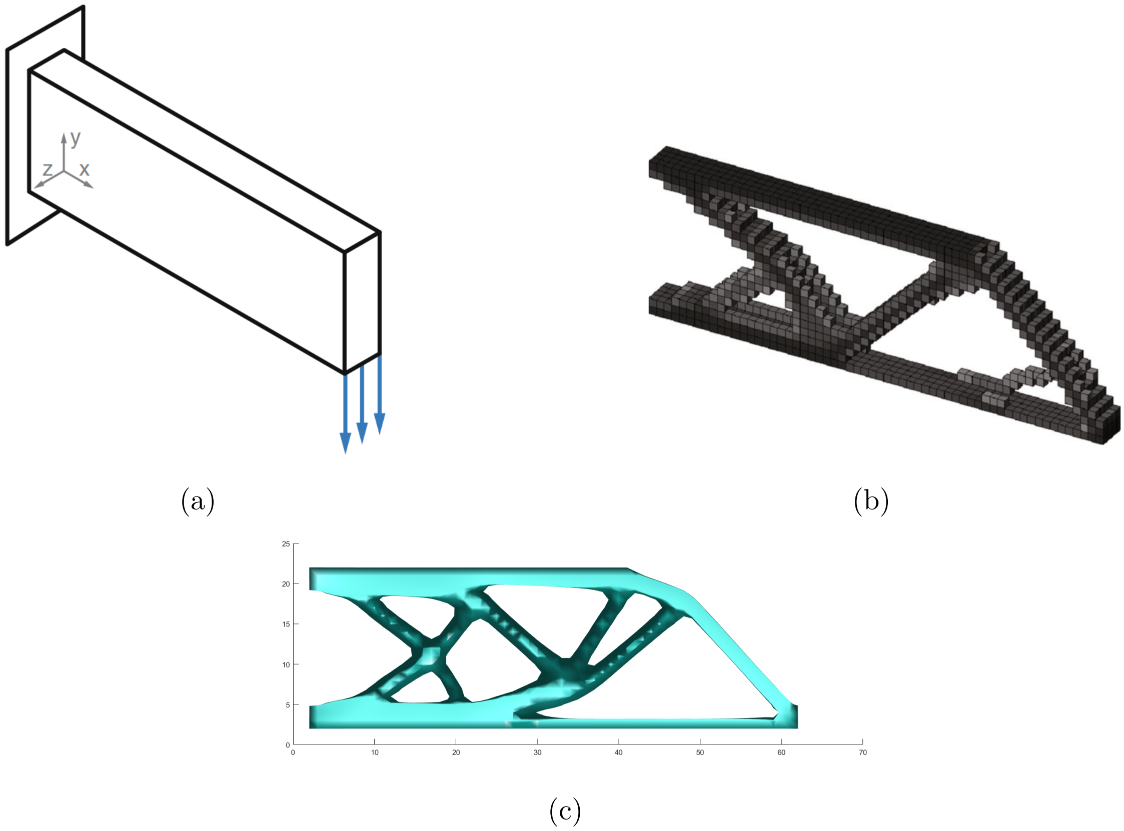

Figure 5.16: Final design comparison. (a) Initial design for both methods. (b) Final Design for SIMP. (c) Final design for GRBF-PLSM

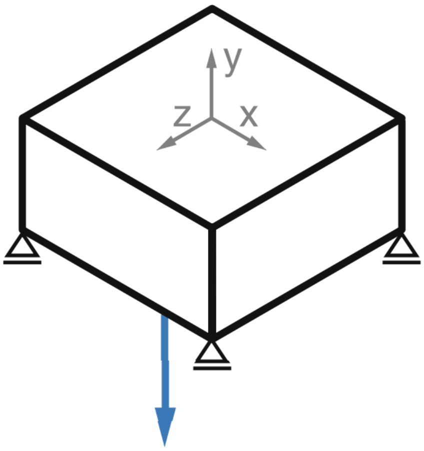

(a)

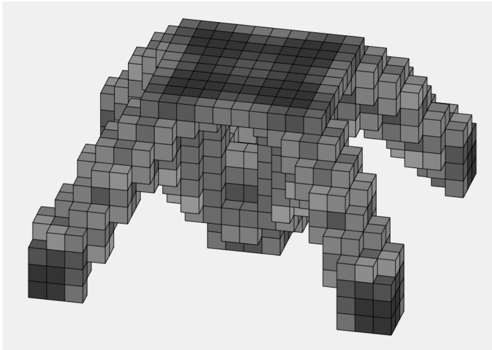

(b)

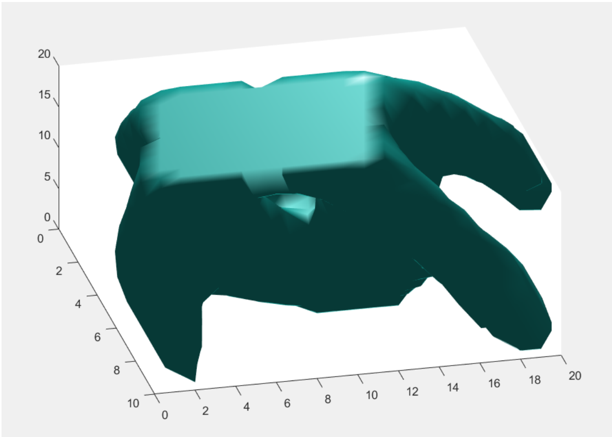

(c)

Figure 5.17: Final design comparison. (a) Initial design for both methods. (b) Final Design for SIMP. (c) Final design for GRBF-PLSM

Chapter 6

Conclusions

6.1 Conclusion

Actors involved in industrial development have always sought to minimize the costs of their activities to maintain their competitiveness in the market. In this way, the manufacturing and operating processes have been continuously improved along with the technological developments over time. In recent decades, the development of computer-aided design software allowed the application of more complex methods of topological optimization to the mechanical design process. Today, there is extensive research and development in structural topological optimization due to the optimal use of material and energy it allows. This optimal use has been highlighted by the United Nations as part of sustainable development.

Topology optimization based on level set methods has become an attractive design tool for obtaining lighter and more efficient structures. This work studied the parameterized level set method for topology optimization for a three-dimensional problem. This method is based on the mathematical simplification of the Hamilton-Jacobi PDE into a more convenient ODEs system. The simplification is performed by parameterizing the level set function by using radial basis functions. Firstly, the boundary of the structure is implicitly represented as the zero level set of a higher-dimensional level set function, and the implicit surface is parameterized through the interpolation of a given set of radial basis functions. In this way, the original Hamilton-Jacobi partial differential equation is transformed into a system of algebraic equations. This review analyzed topology optimization for solid isotropic objects within the framework of compliance minimization. The parameterization approach presented used the GRBF MQ spline due to its performance to approximate functions and smoothness. Along with the review, top3dPLSM was implemented following the method PLSM for topology optimization as an efficient 255 lines MATLAB code.

The features and functionalities of the implemented code satisfy the objectives of this work. `top3dPLSM` uses dedicated MATLAB capabilities for vectorized computation, sparse data processing, and solving systems of equations. As a result, top3dPLSM features a high level of efficiency that enables it to handle reasonably large size and resolution problems.

This code can minimize the compliance of a three-dimensional body subject to customizable boundary conditions. The minimization of the compliance was the first specific objective of our work.

The code includes a plotting routine at each step of the optimization loop. This routine plots the evolution of the surface during the optimization process as well as the value of compliance and the volume of the body. Therefore, the fourth specific objective is met.

top3dPLSM can solve problems with different size configurations, material properties, and boundary conditions. This feature allowed us to replicate previously studied problems presented in literature. In this way, it was possible to compare the results obtained by the code presented in this work and the solutions generated by the implementations presented in other works. Thus, the developed code met the last specific objective.

top3dPLSM is an efficient code, developed to solve three-dimensional topological optimization problems within the framework of compliance minimization and with a volume constraint. It can handle problems with different configurations and provide a live plotting of state variables and optimization process. Therefore, the general objective established for the present work was met.

6.2 Future Work

Structural topology optimization can have a positive impact in almost all industries due to its capabilities to generate high-performance and lightweight structures. United Nations and the Institute for Energy and Environmental Research studied the impact of lightweighting the structures of means of transport. Reducing vehicles weight has the potential to avoid almost 700 million tonnes of carbon dioxide emissions per year from the transport sector. Thus, a natural next step of this research will be studying use cases of topology optimization aimed to reduce the weight of vehicles and their components.

The designing of high-performance structures is being complemented with the integration with additive manufacturing. However, not all optimal designs can be manufactured using additive manufacturing. The optimal design has to be smooth and continuous for its manufacture to be feasible. There are reported methods for topology optimization-based PLSM that consider extrusion constraints aimed to generate 3D pri ntable optimal designs. As future work, we could conduct research aimed to enhance the present implementation to be able to generate additive manufacturing feasible design.

The code presented in this work is capable of performing topological optimization to a 3D elastic isotropic solid body using the parameterized level set method. Globally supported multi-quadratic RBFs were used.

The state of the art of topological optimization based on the parameterized level set method describes approaches that use locally supported RBFs that consume less memory and present a well-conditioned interpolation matrix. It would be interesting to explore this idea as a follow-up work modifying the code to use LRBF.

Additionally, the code uses only CPU and is implicitly parallelized by MATLAB. However, to scale the magnitude of the problems that can be addressed, a code capable of using CPU and GPU processing must be implemented. Thus, we propose to migrate the code to C++ and make use of the PETSc which is the acronym of Portable, Extensible Toolkit for Scientific Computation [56] [57] [58]. PETSC is a suite of tools and data types for scalable parallel solutions of partial differential equations. This suite supports MPI and CUDA. This suite was used by Aage *et al.* for the implementation of a tool for giga-voxel computational morphogenesis for structural design.

6.3 Recommendations

The development of the code presented in this work is the result of the implementation of the method proposed by Wang and Wang in their work Radial basis functions and level set method for structural topology optimization [32]. In this work, the mathematical bases of the method for a 3-dimensional problem are described. However, details regarding its implementation are not mentioned, for this purpose, the work of Liu and Tovar [50] and Wei [55] was used as a reference. In these works, the implementation in MATLAB of the SIMP method for topological optimization for a three-dimensional problem and the implementation of the parameterized level set method for topological optimization for a two-dimensional problem are presented, respectively. The work carried out was, for the most part, to extend the two-dimensional solution presented by Wei, to an implementation capable of solving three-dimensional problems.

In the process of extending Wei's solution [55] to three dimensions, various problems arose, which were resolved through the implementation and validation of different solutions reported as successful in the literature. This was the case of the implementation of the lk_H8 subroutine for the generation of the element stiffness matrix for finite element analysis. This subroutine was presented in the work of Liu and Tovar [50].

The following recommendations are highlighted for the implementation of a solution based on the one presented in this work or for its replication.

- The implementation of a topological optimization algorithm based on the parameterized level set method involves the development and coupling of various components, such as the section that performs topological optimization itself and the section that develops the finite element analysis. For this, it is generally recommended and for each stage of the implementation, to exploit the vectorized computation features that MATLAB offers to simplify the implementation. Additionally, due to the high computational cost inherent to the problem, the use of dedicated tools and functions for vectorized computation allows achieving reasonable computational times depending on the size of the problem. This, in turn, allows you to experiment with objects of larger sizes or with a higher level of detail.

- It is recommended to use algebraic operations between signed distance functions, to generate the initial design of the body to be optimized. This allows for quick deployment and easy debugging. Additionally, it allows generating different initial design configurations without the need to make major changes to the code.

- Take advantage of the built-in functions that MATLAB provides for the development of vectorized algorithms. This is mainly useful when generating the initial layout. At this stage, the repmat, and kron functions are especially useful. As well as bsxfun, which allows mapping functions to vectors.

- A simple design to generate and that has been useful for the work presented is to initialize a parallelepiped with zero values and later replace the values of an internal inscribed parallelepiped of three units less in each dimension with an ascending number pattern in each direction. corresponding to the x, y, z axes.

- It is recommended to use the shape parameter cRBF = 1e-5 for all the radial basis functions used. This value has been used successfully in different related implementations.

- It is recommended to use the MATLAB linear systems solver operator to solve the equation: 2.22. This is because it is numerically possible that the matrix involved is badly conditioned, that is, almost singular. MATLAB will detect this and use an iterative method to solve this system of linear equations.

- It is recommended to implement a function that generates the loads and supports defined by the user. This is because the implementation of these components can be abstracted, thus reducing the complexity of the configuration of the loads and supports mentioned.

- In the implementation of finite element analysis, it is recommended to use the same material properties of this study. These parameters have been widely used in various studies, thus allowing a consistent comparison of results as well as allowing expected behavior.

- For a simple implementation and easy to compare with other jobs, it is recommended to use the lk_H8 subroutine. This function was proposed by Liu and Tovar [6] and is in charge of generating the element stiffness matrix KE. This function receives as its only parameter the coefficient nu and is used for all the elements that make up the object.

- Due to the large number of elements contained in the matrices involved in the equilibrium equation, it is recommended to use sparse matrices to store these values. The use of dedicated structures for storing sparse matrices is especially relevant due to the enormous amount of data, most of which is 0.

- When defining the parameters involved in the optimization loop, it is recommended to define a maximum number of iterations large enough to allow the convergence of the solution and for it to meet the stop condition. Likewise, the time step size must be small enough to maintain numerical stability and be consistent with the CFL condition.

- It is recommended to generate a visualization of the orthogonality conditions of the interpolation of the radial basis function to verify compliance with these conditions.

- It is recommended to configure the stop condition as a combination of volume convergence and compliance achieved. That is, if the object has a compliance variation less than 1e-3 in the last 9 iterations and the volume constraint has already been met, the optimization iteration will stop.

- It is recommended to implement the fuzzy reset scheme. This increases numerical stability and allows for earlier convergence.

- Finally, it is recommended to implement post-processing to the result obtained from the main routine. This is since being a level set method, only the level set zero can be displayed, therefore, only the values equal to zero, or failing that, intermediate values between a positive and negative number, would be represented as part of the final object.

Bibliography

[1] M. Bendsoe and O. Sigmund, *Topology Optimization: Theory, Methods, and Applications*, ser. Engineering online library. Springer Berlin Heidelberg, 2003. [Online]. Available: https://books.google.com.ec/books?id=NGmtmMhVe2sC

[2] P. Wei, Z. Li, X. Li, and M. Y. Wang, "An 88-line matlab code for the parameterized level set method based topology optimization using radial basis functions," *Structural and Multidisciplinary Optimization*, vol. 58, no. 2, pp. 831–849, Aug 2018. [Online]. Available: https://doi.org/10.1007/s00158-018-1904-8

[3] H. Deng and A. C. To, "A parametric level set method for topology optimization based on deep neural network (dnn)," 2021.

[4] "3d printing for aerospace with eos technology." [Online]. Available: https://www.eos.info/en/3d-printing-examples-applications/all-3d-printing-applications/ruag-aerospace-3d-printed-satellite-components

[5] S. ul Islam, W. Khan, B. Ullah, and Z. Ullah, "The localized radial basis functions for parameterized level set based structural optimization," *Engineering Analysis with Boundary Elements*, vol. 113, Feb. 2020.

[6] K. Liu and A. Tovar, "An efficient 3d topology optimization code written in matlab," *Structural and Multidisciplinary Optimization*, vol. 50, no. 6, pp. 1175–1196, Dec 2014. [Online]. Available: https://doi.org/10.1007/s00158-014-1107-x

[7] N. Aage, E. Andreassen, B. S. Lazarov, and O. Sigmund, "Giga-voxel computational morphogenesis for structural design," *Nature*, vol. 550, no. 7674, pp. 84–86, Oct 2017. [Online]. Available: https://doi.org/10.1038/nature23911

[8] H. Helms and U. Lambrecht, "The potential contribution of light-weighting to reduce transport energy consumption," *The International Journal of Life Cycle Assessment*, August 2007.

[9] W. Bank, "Carbon pricing dashboard."

[10] H. Helms and U. Lambrecht, "Energy savings by lightweighting." 2004.

[11] ——, "Energy savings by light-weighting - ii." 2004.

[12] H. Helms and J. Kräck, "Energy savings by light-weighting - 2016 update," December 2016.

[13] K. Dube and G. Nhamo, *Major Global Aircraft Manufacturers and Emerging Responses to the SDGs Agenda*. Cham: Springer International Publishing, 2020, pp. 99–113. [Online]. Available: https://doi.org/10.1007/978-3-030-33216-7_7

[14] H. Li, P. Li, L. Gao, L. Zhang, and T. Wu, "A level set method for topological shape optimization of 3d structures with extrusion constraints," *Computer Methods in Applied Mechanics and Engineering*, vol. 283, pp. 615–635, 2015. [Online]. Available: https://www.sciencedirect.com/science/article/pii/S0045782514003764

[15] S. Osher and R. Fedkiw, *The Level Set Methods and Dynamic Implicit Surfaces*. Springer, New York, NY, 05 2004, vol. 57.

[16] S. Osher and J. A. Sethian, "Fronts propagating with curvature-dependent speed: Algorithms based on hamilton-jacobi formulations," *Journal of Computational Physics*, vol. 79, no. 1, pp. 12–49, 1988. [Online]. Available: https://www.sciencedirect.com/science/article/pii/0021999188900022

[17] D. Peng, B. Merriman, S. Osher, H. Zhao, and M. Kang, "A pde-based fast local level set method," *Journal of Computational Physics*, vol. 155, no. 2, pp. 410–438, 1999. [Online]. Available: https://www.sciencedirect.com/science/article/pii/S0021999199963453

[18] J. Sethian, "Level set methods and fast marching methods," *Cambridge Monographs on Applied and Computational Mathematics*, vol. 37, 1999.

[19] M. Burger, B. Hackl, and W. Ring, "Incorporating topological derivatives into level set methods," *Journal of Computational Physics*, vol. 194, pp. 344–362, 07 2004.

[20] N. H. Kim and Y. Chang, "Eulerian shape design sensitivity analysis and optimization with a fixed grid," *Computer Methods in Applied Mechanics and Engineering*, vol. 194, no. 30, pp. 3291–3314, 2005, structural and Design Optimization. [Online]. Available: https://www.sciencedirect.com/science/article/pii/S0045782505000484

[21] E. Kansa, "Multiquadrics—a scattered data approximation scheme with applications to computational fluid-dynamics—i surface approximations and partial derivative estimates," *Computers Mathematics with Applications*, vol. 19, no. 8, pp. 127–145, 1990. [Online]. Available: https://www.sciencedirect.com/science/article/pii/089812219090270T

[22] J. A. Sethian, *Level set methods and fast marching methods: evolving interfaces in computational geometry, fluid mechanics, computer vision, and materials science*. Cambridge university press, 1999, vol. 3.

[23] M. Burger, B. Hackl, and W. Ring, "Incorporating topological derivatives into level set methods," *Journal of Computational Physics*, vol. 194, no. 1, pp. 344–362, 2004. [Online]. Available: https://www.sciencedirect.com/science/article/pii/S0021999103004868

[24] G. Allaire, F. de gournay, F. Jouve, and A.-M. Toader, “Structural optimization using topological and shape sensitivity via a level set method,” *Control and Cybernetics*, vol. 34, 01 2005.

[25] J. C. Carr, R. K. Beatson, J. B. Cherrie, T. J. Mitchell, W. R. Fright, B. C. McCallum, and T. R. Evans, “Reconstruction and representation of 3d objects with radial basis functions,” in *Proceedings of the 28th Annual Conference on Computer Graphics and Interactive Techniques*, ser. SIGGRAPH ’01. New York, NY, USA: Association for Computing Machinery, 2001, p. 67–76. [Online]. Available: https://doi.org/10.1145/383259.383266

[26] Q. J. L. . O. S. Cecil, T., “Numerical methods for high dimensional hamilton-jacobi equations using radial basis functions,” *Journal of Computational Physics*, pp. 327–347, 2004. [Online]. Available: https://escholarship.org/uc/item/16311645

[27] A. Cheng, M. Golberg, E. Kansa, and G. Zammito, “Exponential convergence and h-c multiquadric collocation method for partial differential equations,” *Numerical Methods for Partial Differential Equations*, vol. 19, pp. 571 – 594, 09 2003.

[28] E. Kansa, H. Power, G. Fasshauer, and L. Ling, “A volumetric integral radial basis function method for time-dependent partial differential equations. i. formulation,” *Engineering Analysis with Boundary Elements*, vol. 28, no. 10, pp. 1191–1206, 2004, mesh Reduction Technique Part II. [Online]. Available: https://www.sciencedirect.com/science/article/pii/S095579970400013X

[29] C. A. Micchelli, “Interpolation of scattered data: Distance matrices and conditionally positive definite functions, volume = 19, journal = Constructive Approximation, doi = 10.1007/BF01893414,” pp. 571 – 594, 12 1986.

[30] R. Franke, “Scattered data interpolation: Tests of some method,” *Mathematics of Computation*, vol. 38, no. 157, pp. 181–200, 1982. [Online]. Available: http://www.jstor.org/stable/2007474

[31] B. Morse, T. Yoo, P. Rheingans, D. Chen, and K. Subramanian, “Interpolating implicit surfaces from scattered surface data using compactly supported radial basis functions,” in *Proceedings International Conference on Shape Modeling and Applications*, 2001, pp. 89–98.

[32] S. Wang and M. Y. Wang, “Radial basis functions and level set method for structural topology optimization,” *International Journal for Numerical Methods in Engineering*, vol. 65, no. 12, pp. 2060–2090, 2006. [Online]. Available: https://onlinelibrary.wiley.com/doi/abs/10.1002/nme.1536

[33] M. D. Buhmann, *Radial Basis Functions: Theory and Implementations*, ser. Cambridge Monographs on Applied and Computational Mathematics. Cambridge University Press, 2003.

[34] E. Kansa, H. Power, G. Fasshauer, and L. Ling, “A volumetric integral radial basis function method for time-dependent partial differential equations. i. formulation,” *Engineering Analysis With Boundary Elements*, vol. 28, pp. 1191–1206, 2004.

[35] D. F. Richards, M. O. Bloomfield, S. Sen, and T. S. Cale, "Extension velocities for level set based surface profile evolution," *Journal of Vacuum Science & Technology A*, vol. 19, no. 4, pp. 1630–1635, 2001. [Online]. Available: https://doi.org/10.1116/1.1380230

[36] J. C. Carr, R. K. Beatson, J. B. Cherrie, T. J. Mitchell, W. R. Fright, B. C. McCallum, and T. R. Evans, "Reconstruction and representation of 3d objects with radial basis functions," p. 67–76, 2001. [Online]. Available: https://doi.org/10.1145/383259.383266

[37] M. Y. Wang, X. Wang, and D. Guo, "A level set method for structural topology optimization," *Computer Methods in Applied Mechanics and Engineering*, vol. 192, no. 1, pp. 227–246, 2003. [Online]. Available: https://www.sciencedirect.com/science/article/pii/S0045782502005595

[38] S. Wang and M. Y. Wang, "Radial basis functions and level set method for structural topology optimization," *International Journal for Numerical Methods in Engineering*, vol. 65, no. 12, pp. 2060–2090, 2006. [Online]. Available: https://onlinelibrary.wiley.com/doi/abs/10.1002/nme.1536

[39] B. Wang, Y. Zhou, Y. Zhou, S. Xu, and B. Niu, "Diverse competitive design for topology optimization," *Structural and Multidisciplinary Optimization*, vol. 57, no. 2, pp. 891–902, Feb 2018. [Online]. Available: https://doi.org/10.1007/s00158-017-1762-9

[40] J. ZHU, H. ZHOU, C. WANG, L. ZHOU, S. YUAN, and W. ZHANG, "A review of topology optimization for additive manufacturing: Status and challenges," *Chinese Journal of Aeronautics*, vol. 34, no. 1, pp. 91–110, 2021. [Online]. Available: https://www.sciencedirect.com/science/article/pii/S1000936120304520

[41] M. Raissi, P. Perdikaris, and G. Karniadakis, "Physics-informed neural networks: A deep learning framework for solving forward and inverse problems involving nonlinear partial differential equations," *Journal of Computational Physics*, vol. 378, pp. 686–707, 2019. [Online]. Available: https://www.sciencedirect.com/science/article/pii/S0021999118307125

[42] R. Iten, T. Metger, H. Wilming, L. del Rio, and R. Renner, "Discovering physical concepts with neural networks," *Physical Review Letters*, vol. 124, no. 1, Jan 2020. [Online]. Available: http://dx.doi.org/10.1103/PhysRevLett.124.010508

[43] S. L. Brunton, B. R. Noack, and P. Koumoutsakos, "Machine learning for fluid mechanics," *Annual Review of Fluid Mechanics*, vol. 52, no. 1, pp. 477–508, 2020. [Online]. Available: https://doi.org/10.1146/annurev-fluid-010719-060214

[44] M. Raissi, Z. Wang, M. S. Triantafyllou, and G. E. Karniadakis, "Deep learning of vortex-induced vibrations," *Journal of Fluid Mechanics*, vol. 861, p. 119–137, Dec 2018. [Online]. Available: http://dx.doi.org/10.1017/jfm.2018.872

[45] Y. Yu, T. Hur, J. Jung, and I. G. Jang, "Deep learning for determining a near-optimal topological design without any iteration," *Structural and Multidisciplinary Optimization*, vol. 59, no. 3, pp. 787–799, Mar 2019. [Online]. Available: https://doi.org/10.1007/s00158-018-2101-5

[46] X. Lei, C. Liu, Z. Du, W. Zhang, and X. Guo, "Machine Learning-Driven Real-Time Topology Optimization Under Moving Morphable Component-Based Framework," *Journal of Applied Mechanics*, vol. 86, no. 1, 10 2018, 011004. [Online]. Available: https://doi.org/10.1115/1.4041319

[47] S. Wang, K. Lim, B. Khoo, and M. Wang, "An extended level set method for shape and topology optimization," *Journal of Computational Physics*, vol. 221, no. 1, pp. 395–421, 2007. [Online]. Available: https://www.sciencedirect.com/science/article/pii/S0021999106002968

[48] S. ul Islam and I. Ahmad, "A comparative analysis of local meshless formulation for multi-asset option models," *Engineering Analysis with Boundary Elements*, vol. 65, pp. 159–176, 2016. [Online]. Available: https://www.sciencedirect.com/science/article/pii/S0955799716000175

[49] B. Šarler and R. Vertnik, "Meshfree explicit local radial basis function collocation method for diffusion problems," *Computers Mathematics with Applications*, vol. 51, no. 8, pp. 1269–1282, 2006, radial Basis Functions and Related Multivariate Meshfree Approximation Methods: Theory and Applications. [Online]. Available: https://www.sciencedirect.com/science/article/pii/S0898122106000836

[50] Y. Liu, Z. Li, P. Wei, and W. Wang, "Parameterized level-set based topology optimization method considering symmetry and pattern repetition constraints," *Computer Methods in Applied Mechanics and Engineering*, vol. 340, pp. 1079–1101, 2018. [Online]. Available: https://www.sciencedirect.com/science/article/pii/S0045782518302135

[51] G. Yao, J. Duo, C. Chen, and L. Shen, "Implicit local radial basis function interpolations based on function values," *Applied Mathematics and Computation*, vol. 265, pp. 91–102, 2015. [Online]. Available: https://www.sciencedirect.com/science/article/pii/S009630031500569X

[52] Z. Luo, L. Tong, and Z. Kang, "A level set method for structural shape and topology optimization using radial basis functions," *Computers Structures*, vol. 87, no. 7, pp. 425–434, 2009. [Online]. Available: https://www.sciencedirect.com/science/article/pii/S0045794909000273

[53] G. Allaire, F. Jouve, and A.-M. Toader, "Structural optimization using sensitivity analysis and a level-set method," *Journal of Computational Physics*, vol. 194, no. 1, pp. 363–393, 2004. [Online]. Available: https://www.sciencedirect.com/science/article/pii/S002199910300487X

[54] X. Xie and M. Mirmehdi, "Radial basis function based level set interpolation and evolution for deformable modelling," *Image Vision Comput.*, vol. 29, no. 2–3, p. 167–177, Feb. 2011. [Online]. Available: https://doi.org/10.1016/j.imavis.2010.08.011

[55] P. Wei, Z. Li, X. Li, and M. Y. Wang, "An 88-line matlab code for the parameterized level set method based topology optimization using radial basis functions," *Structural and Multidisciplinary Optimization*, vol. 58, pp. 831–849, 2018.

[56] S. Balay, S. Abhyankar, M. F. Adams, J. Brown, P. Brune, K. Buschelman, L. Dalcin, A. Dener, V. Eijkhout, W. D. Gropp, D. Kaushik, M. G. Knepley, D. A. May, L. C. McInnes, R. T. Mills, T. Munson, K. Rupp, P. Sanan, B. F. Smith, S. Zampini, H. Zhang, and H. Zhang, "PETSc Web page," 2021, https://petsc.org/.

[57] ——, "PETSc users manual," Argonne National Laboratory, Tech. Rep. ANL-95/11 - Revision 3.15, 2021.

[58] S. Balay, W. D. Gropp, L. C. McInnes, and B. F. Smith, "Efficient management of parallelism in object oriented numerical software libraries," in *Modern Software Tools in Scientific Computing*, E. Arge, A. M. Bruaset, and H. P. Langtangen, Eds. Birkhauser Press, 1997, pp. 163–202.